RECLAMATION

Managing Water in the West

Technical Memorandum TM-85-833000-2016-10

2015 Annual Report
Paradox Valley Seismic Network
Paradox Valley Unit, Colorado

U.S. Department of the Interior
Bureau of Reclamation

May 2016

Mission Statements

The mission of the Department of the Interior is to protect and provide access to our Nation's natural and cultural heritage and honor our trust responsibilities to Indian Tribes and our commitments to island communities.

The mission of the Bureau of Reclamation is to manage, develop, and protect water and related resources in an environmentally and economically sound manner in the interest of the American public.

BUREAU OF RECLAMATION
Technical Service Center, Denver, Colorado
Seismology, Geomorphology, and Geophysics Group

Technical Memorandum TM-85-833000-2016-10

2015 Annual Report
Paradox Valley Seismic Network
Paradox Valley Unit, Colorado

Prepared by:

Lisa Block, Geophysicist — Date: 5/18/2016

Mark Meremonte, Geophysicist — Date: 5/18/2016

Vanessa King, Geophysicist — Date: 5/18/16

Christopher Wood, Geophysicist — Date: 5/18/2016

Peer Review Certification
This report has been reviewed and is believed to be in accordance with the service agreement and standards of the profession.

Peer reviewed by:

Glenda Besana-Ostman, Geophysicist — Date: 5-18-2016

Acknowledgements

The work described in this report and the continuous operation of the Paradox Valley Seismic Network are made possible through the considerable assistance and support of Andy Nicholas, site Project Manager at the Paradox Valley Unit, Bedrock, CO. Mike Gilliam, Justin Schwarzer, and Matthew Jones (Reclamation, Denver, CO) provided essential field support. Scott Cartwright provided valuable IT support of the production data acquisition computer systems. We thank Brad McKinney, Nucla Airport Manager, for supporting our operations there.

Contents

Page

1 Introduction 1

2 Project Background 3
2.1 Paradox Valley Unit 3
2.2 PVU Injection Operations 7
2.2.1 Phase I (July 22, 1996 – July 25, 1999) 7
2.2.2 Phase II (July 26, 1999 – June 22, 2000) 9
2.2.3 Phase III (June 23, 2000 – January 6, 2002) 9
2.2.4 Phase IV (January 7, 2002 – April 16, 2013) 9
2.2.5 Phase V (April 17, 2013 – present) 10
2.3 Seismic Monitoring 11
2.3.1 Paradox Valley Seismic Network 11
2.3.2 Induced Seismicity 17

3 Network Operations 21
3.1 Network Maintenance and Upgrades 21
3.2 Network Performance 21
3.3 Data Acquisition Software Transition Testing 23

4 Seismic Data Recorded in 2015 29
4.1 Annual Summary 29
4.2 Shallow Earthquakes within 10 km of the Injection Well 35
4.2.1 2015 Seismicity 35
4.2.2 Comparison to 2014 Seismicity 38
4.3 Distant Earthquakes 40
4.4 Historical Seismicity Trends 40

5 Conclusions 45

6 References 47

2015 Site Visit Report ..... Appendix A
Evaluation of PVSN Event Detection ..... Appendix B
PVSN 2015 Local Earthquake Catalog ..... Appendix C

Tables

Page

Table 2-1: PVSN Station Locations and Characteristics 16
Table 2-2: PVSN Telemetered Sites - Station Location Names 17
Table 3-1: Performance of PVSN seismic stations during 2015 24
Table 3-2: PVSN station uptime in 2015. 27
Table 3-3: Times when PVSN data acquisition was down or degraded in 2015 28
Table 3-4: Annual PVSN data acquisition uptime 28
Table 4-1: Summary of events recorded during 2015 by old event location categories 33
Table 4-2: Summary of events recorded during 2015 by new event location categories 33

Figures

Page

Figure 2-1. Location of the deep injection well at Reclamation's Paradox Valley Unit in western Colorado. 4
Figure 2-2. Location of the Paradox Valley Unit extraction wells and injection well. 5
Figure 2-3. Vertical cross section roughly perpendicular to Paradox Valley, looking to the northwest. The location of the cross section is shown in Figure 2 2. Based on figure from Bremkamp and Harr (1988). 6
Figure 2-4: PVU injection well in plan view (left) and north-viewing vertical cross section (right). Figures include the near-wellbore stratigraphy and locations of the upper and lower casing perforations. 6
Figure 2-5: Daily average injection flow rate, daily average surface injection pressure, daily average downhole pressure at 4.3 km depth, and cumulative volume of brine injected during PVU injection operations. 8
Figure 2-6: Stacked multi-taper acceleration power spectra from the east-west components of Guralp model CMG40TD seismometers installed at four first-generation stations near Hungry Horse Dam, Montana. Figure from O'Connell (2008). 13
Figure 2-7: Locations of the PVSN seismic stations, PVU injection well, and epicenters of earthquakes less than 8.5 km deep. Physiographic provinces from Fenneman and Johnson (1946). 15
Figure 2-8: Lower plot: scatter plot of earthquakes having magnitude ≥ 0.5 and depth < 8.5 km (relative to the ground surface elevation at the injection wellhead), plotted as a function of date and distance from the PVU injection well. Upper plot: daily average injection flow rate. 18
Figure 2-9: Maps showing the spatial distribution of shallow seismicity recorded in the Paradox Valley area over time: (a) injection tests, 1991-1995 (b) continuous injection,1996-2000 (c) continuous injection, 2001-2008 (d) continuous injection, 2009-2015. All earthquakes less than 8.5 km deep (relative to the ground surface elevation at the injection wellhead) are included. ... 19
Figure 3-1: Daily uptime (%) for each PVSN seismic station during 2015. Vertical axes on plots are scaled from 0 to 115%. 25
Figure 3-2: Same as Figure 3-1 for the rest of the PVSN stations. Bottom plot shows the daily average performance for all PVSN stations. 26
Figure 3-3. Graph of annual (2015) uptime for each PVSN seismic station. 27

Figure 4-1: Locations of local earthquakes recorded by PVSN during 2015 and previous years. The events that occurred during 2015 are color-coded using the old event location categories. . 31
Figure 4-2: Locations of local earthquakes recorded by PVSN during 2015 and previous years. The events that occurred during 2015 are color-coded using the new event location categories. 32
Figure 4-3: Earthquakes recorded by PVSN during 2015, plotted as a function of date, magnitude, and old event location categories.. 34
Figure 4-4: Earthquakes recorded by PVSN during 2015, plotted as a function of date, magnitude, and new event location categories.. 34
Figure 4-5: Map showing the epicenters of shallow earthquakes (< 8.5 km depth) in the vicinity of the injection well in 2015, compared to the locations of previously-induced events..... 36
Figure 4-6: Vertical cross sections showing the hypocenters of earthquakes occurring within approximately 10 km of the injection well in 2015, compared to the locations of previously-induced events: (a) section parallel to Paradox Valley (b) section perpendicular to Paradox Valley.. 37
Figure 4-7: Magnitude histograms of events within 5 km of the injection well (top), at distances of 5 to 10 km from the well (middle), and in both regions (bottom) during 2015 and 2014..... 39
Figure 4-8: Injection well downhole pressure data averaged over daily, 6-month, 18-month, and 30-month time periods (a) and occurrence of shallow seismicity (depth < 10 km) as a function of date and magnitude within 5 km of the injection well (b), at distances of 5 to 10 km from the well (c), and more than 10 km from the well (d). 42
Figure 4-9: Same as Figure 4-8, but only showing data from 2008-2015. 43
Figure 4-10: Annual number of shallow earthquakes (depth < 10 km) with $M_D \geq 0.5$ within 5 km of the injection well (a), 5 to 10 km from the well (b), and more than 10 km from the well (c). Data from 2008 to 2015 are shown. 44

1 Introduction

The Paradox Valley Seismic Network (PVSN) monitors earthquakes induced by injection operations at the Bureau of Reclamation's Paradox Valley Unit (PVU) deep disposal well, as well as local naturally occurring earthquakes. This report summarizes PVSN operations and the data recorded during calendar year 2015. We provide project background information in section 2, including the history of PVU injection operations and details of the seismic network. In section 3, we present PVSN network operations during 2015, including maintenance of the seismic stations and data acquisition systems and annual network performance. The earthquake data recorded during 2015 are discussed in section 4 and compared to historical seismicity trends.

2 Project Background

2.1 Paradox Valley Unit

Reclamation's Paradox Valley Unit (PVU), a component of the Colorado River Basin Salinity Control Project, intercepts salt brine that would otherwise flow into the Dolores River, a tributary of the Colorado River. PVU is located in western Montrose County approximately 90 km southwest of Grand Junction, CO and 16 km east of the Colorado-Utah border (Figure 2-1). The Dolores River flows from southwest to northeast across Paradox Valley (Figure 2-2), which was formed by the collapse of a salt-cored anticline (Figure 2-3). Due to the presence of the salt diapir underlying Paradox Valley, groundwater within the valley is nearly eight times more saline than ocean water. To prevent this highly saline groundwater from entering the Dolores River and degrading water quality downstream, the brine is extracted from nine shallow wells located within the valley near the river. The diverted brine is injected at high pressure into a deep disposal well, designated as PVU Salinity Control Well No. 1. The disposal well is located approximately 1.5 km southwest of Paradox Valley, near the town of Bedrock (Figure 2-2).

PVU Salinity Control Well No. 1 was completed in 1987 at a total depth of 4.88 km (approximately 16,000 ft). The well was built to Environmental Protection Agency (EPA) Underground Injection Code (UIC) Class I standards ("Isolate hazardous, industrial and municipal wastes through deep injection"), but was permitted in 1995 by EPA as a Class V disposal well ("Manage the shallow injection of non-hazardous fluids"). The well penetrates Triassic- through Cambrian-age sedimentary rock layers and granitic Precambrian basement (Figure 2-3). Based on interpretation of regional core and log data, the Mississippian Leadville carbonate was selected as the primary injection zone with the upper Precambrian as a secondary zone (Bremkamp and Harr, 1988). The overlying Paradox salt formation acts as a confining layer. The well casing of PVU No. 1 (constructed of Hastelloy C- 276, a nickel-molybdenum-chromium alloy) was perforated at a spacing of ~20 perforations per meter in two major intervals between 4.3 km and 4.8 km depth. Plan and vertical views of the wellbore, with near-wellbore stratigraphy and the perforation intervals, are shown in Figure 2-4.

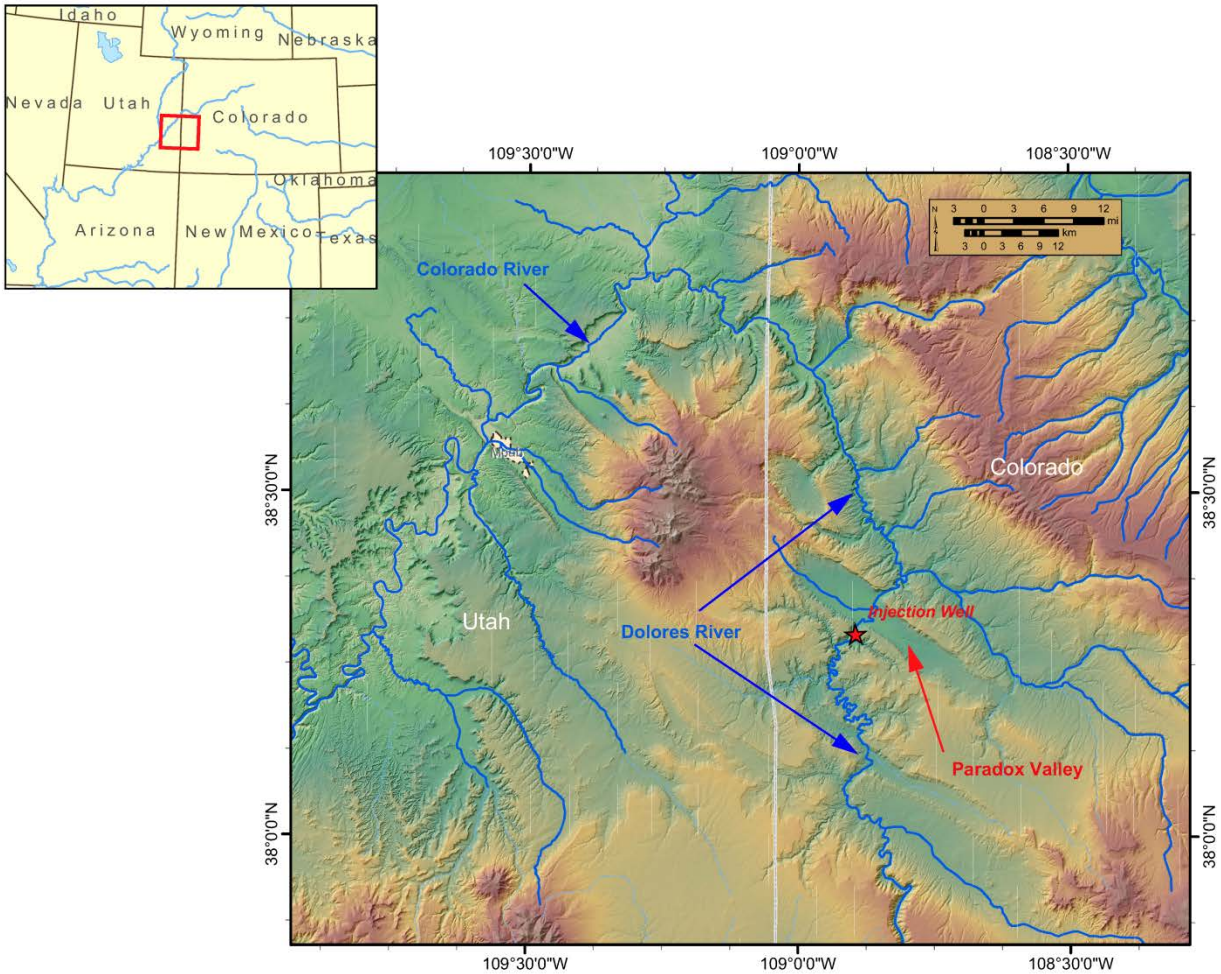

Figure 2-1. Location of the deep injection well at Reclamation's Paradox Valley Unit in western Colorado.

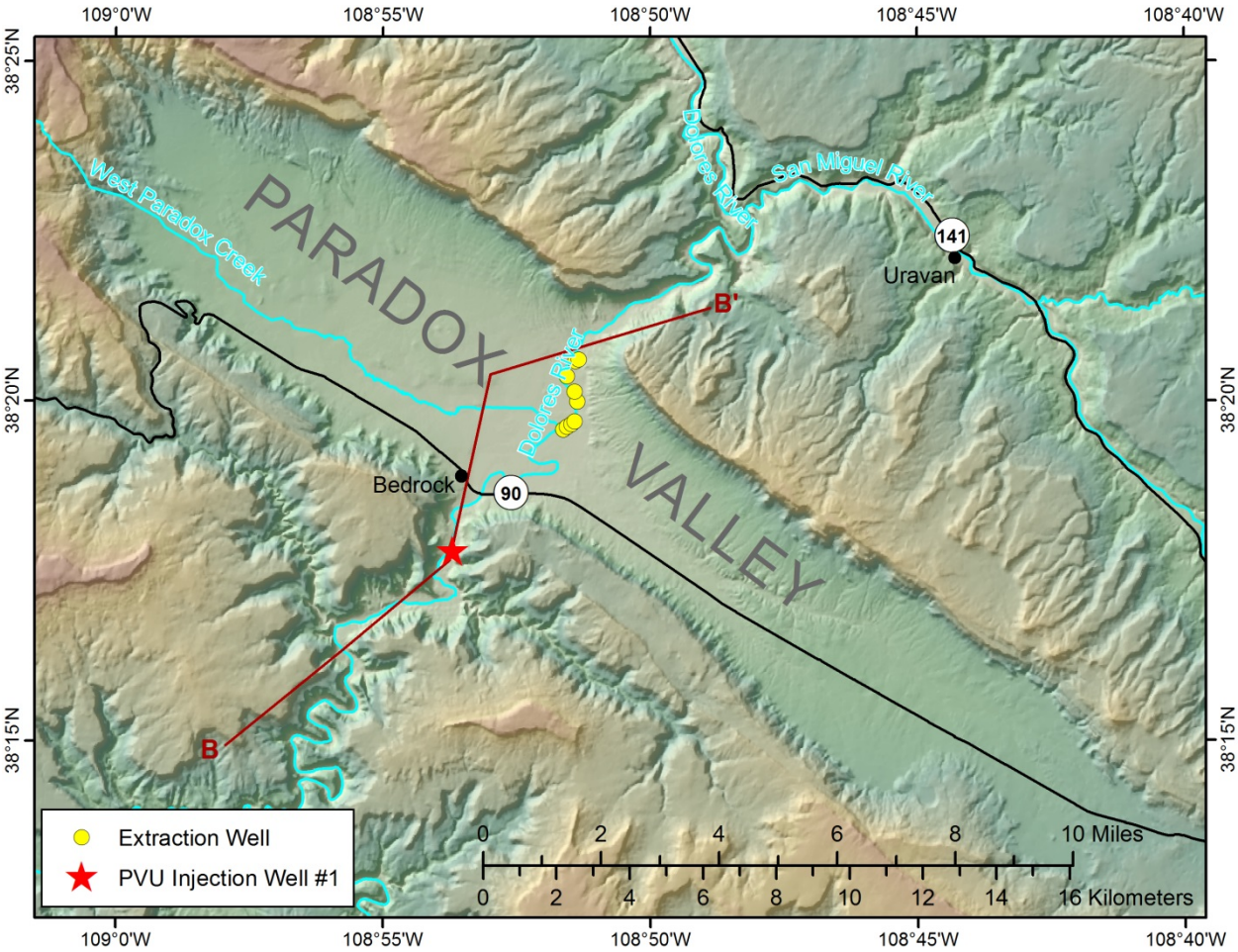

Figure 2-2. Location of the Paradox Valley Unit extraction wells (yellow circles) and injection well (red star). Cross section B-B´ is shown in Figure 2-3.

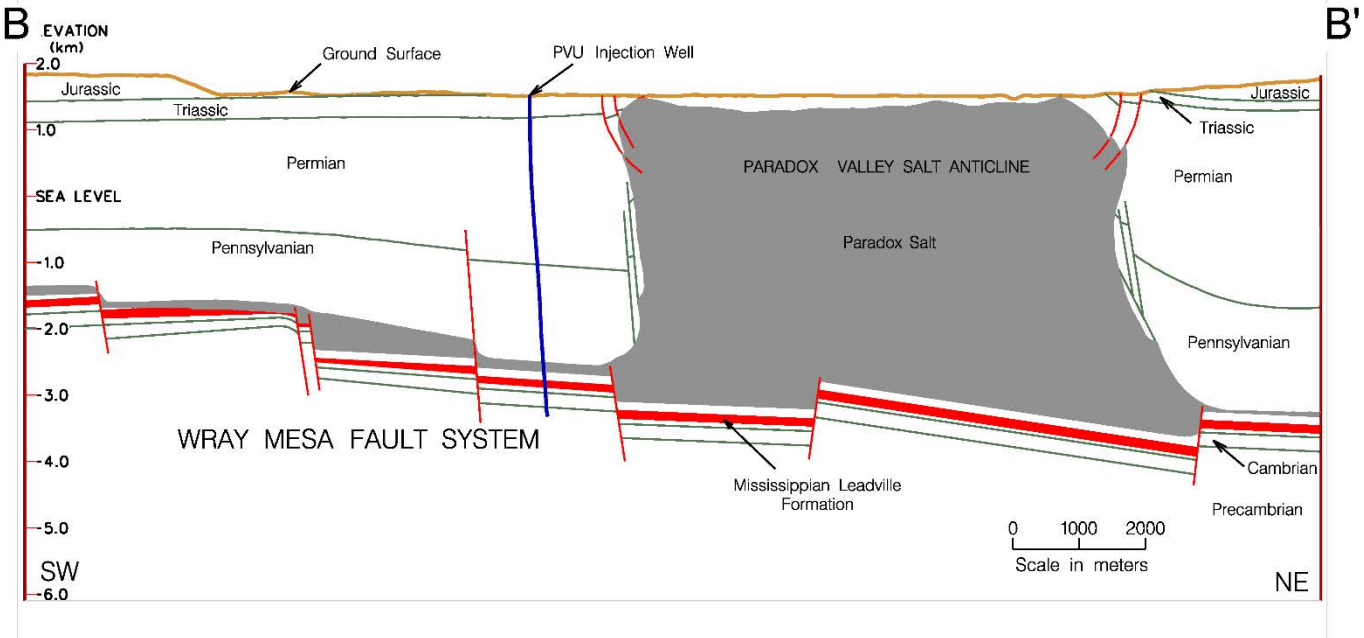

Figure 2-3. Vertical cross section roughly perpendicular to Paradox Valley, looking to the northwest. The location of the cross section is shown in Figure 2 2. Based on figure from Bremkamp and Harr (1988).

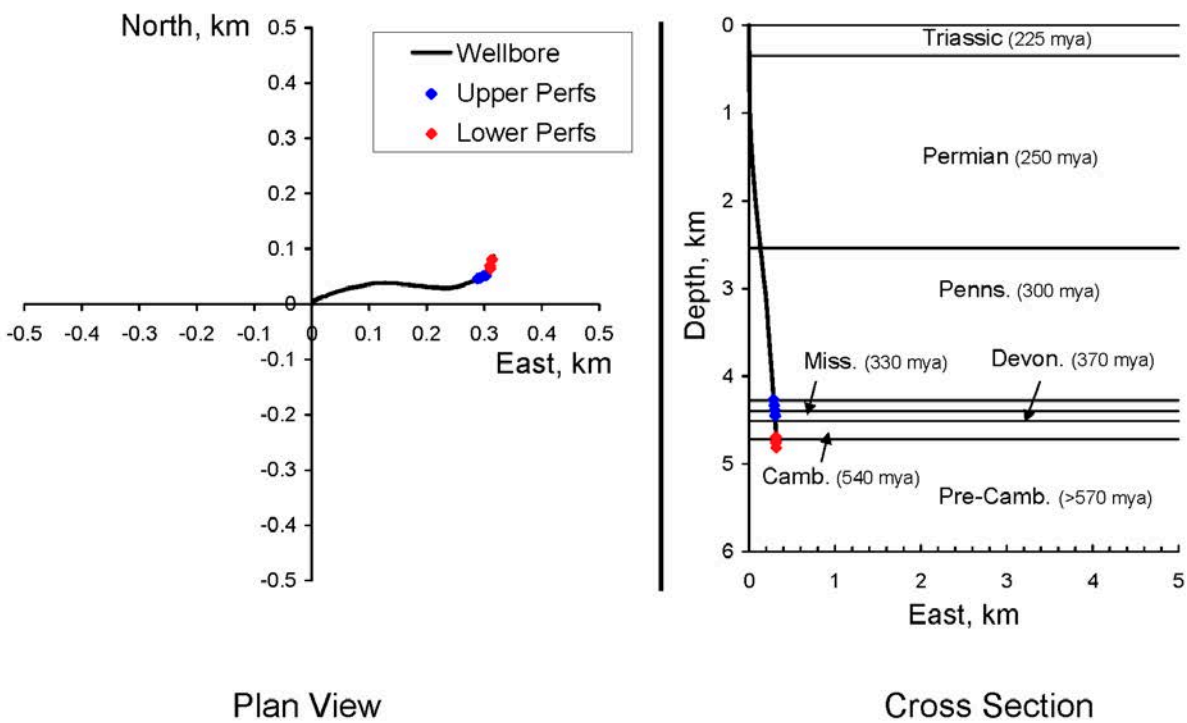

Figure 2-4: PVU injection well in plan view (left) and north-viewing vertical cross section (right). Figures include the near-wellbore stratigraphy and locations of the upper and lower casing perforations.

2.2 PVU Injection Operations

Between 1991 and 1995, Reclamation conducted a series of seven injection tests, an acid stimulation test, and a reservoir integrity test at PVU. The purpose of these tests was to qualify for a Class V permit for deep disposal from the EPA. Near-continuous, long-term disposal of brine began in July 1996, after EPA granted the permit. Since long-term injection began, Reclamation has instituted and maintained four major changes in injection operations. Each change was invoked to mitigate the potential for unacceptable seismicity or to improve injection economics. Each change was maintained for a sufficient period to be considered a sustained injection "phase". These injection phases are described below. Plots of the daily average injection flow rates, daily average surface injection pressures, daily average downhole pressures (at a depth of 4.3 km), and cumulative injected fluid volumes during PVU injection operations are shown in Figure 2-5. The downhole
pressures shown were computed from measured surface pressures using the density of the brine column in the wellbore.

2.2.1 Phase I (July 22, 1996 – July 25, 1999)

During this initial phase of continuous injection, PVU injected at a nominal flow rate of 345 gpm (~1306 l/min), at about 4,950 psi (~34.1 MPa) average surface pressure. This corresponds to approximately 11,800 psi (~81.4 MPa) downhole pressure at 4.3 km depth. To maintain this flow rate, three constant-rate pumps were used with each operating at 115 gpm. The surface pressure on occasion approached the wellhead pressure safety limit of 5,000 psi. This safety limit is based on the specifications of injection and wellhead equipment. It also corresponds to the maximum allowable surface injection pressure (MASIP) specified in the injection permit issued by EPA, which is specified to prevent breach of the geologic confining layer (the Paradox salt). When the surface pressure approached the MASIP, PVU would shut down one injection pump and sometimes two pumps, reducing the injection rate and allowing the pressure to drop a few hundred psi before returning to a three-pump operation. These shutdowns occurred frequently and lasted for minutes, hours, or a few days. This operational protocol resulted in fairly constant surface and downhole pressures (Figure 2-5). Maintenance shutdowns lasted for one to two weeks and, in mid-1997, a 71-day shutdown was needed to replace operations and maintenance contractors. The shutdowns resulted in an overall average injection rate for *Phase I* of roughly 300 gpm (1136 l/min), and the total of volume of fluid injected was 427 Mgal (1.6×10^9 liters). The injectate during *Phase I* was a mixture of 70% Paradox Valley Brine (PVB) and 30% fresh water.

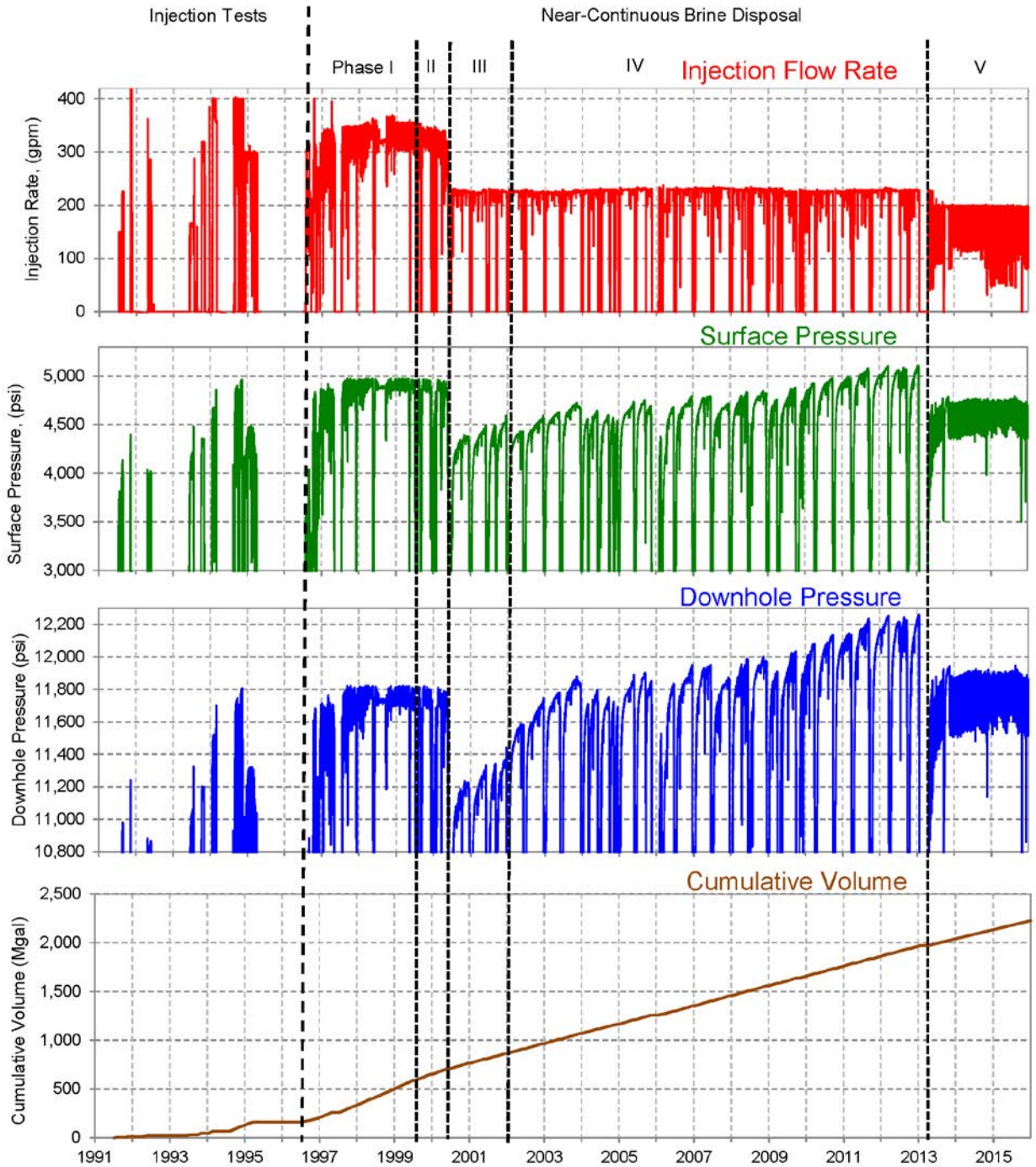

Figure 2-5: Daily average injection flow rate, daily average surface injection pressure, daily average downhole pressure at 4.3 km depth, and cumulative volume of brine injected during PVU injection operations. The downhole pressures are computed from the measured surface pressures using the density of the brine column in the well.

2.2.2 Phase II (July 26, 1999 – June 22, 2000)

Following a local magnitude M_L 3.6 event in June, 1999, and a M_L 3.5 event in July, 1999, PVU altered the injection schedule to include a 20-day shutdown (i.e., a "shut-in") every six months. Prior to these events, it was noted that the rate of seismicity in the near-wellbore region (i.e., within about a 2-km radius from the wellbore) decreased during and following unscheduled maintenance shutdowns and during the shutdowns following the injection tests of 1991 through 1995. It was hypothesized that the biannual shutdowns might reduce the potential for inducing large-magnitude earthquakes by allowing extra time for the injectate to diffuse from the pressurized fractures and faults into the formation rock matrix. When injecting during this phase, the flow rate was the same as during *Phase I*. One hundred and eighteen Mgal (0.4 x 10^9 liters) of fluid was injected during *Phase II*.

2.2.3 Phase III (June 23, 2000 – January 6, 2002)

Immediately following a M_L 4.3 earthquake on May 27, 2000, PVU injection was shut down for 28 days. During this shutdown period, Reclamation evaluated the existing injection strategy and its relationship to induced seismicity. The decision was made to reduce the injection flow rate in the expectation that this change would likely reduce the potential for inducing large-magnitude earthquakes. On June 23, 2000, PVU resumed injection using two pumps rather than alternating between two and three pumps. The biannual 20-day shutdowns were maintained. The nominal flow rate during *Phase III,* while injecting using two pumps, was 230 gpm (~871 l/min). Accounting for the two 20-day shut-ins per year, the average injection flow rate was approximately 205 gpm (776 l/min), a decrease of about 32% compared to *Phase I*. One hundred and fifty-six Mgal (0.6 x 10^9 liters) of fluid was injected during this phase.

2.2.4 Phase IV (January 7, 2002 – April 16, 2013)

Beginning with continuous injection operations in 1996, PVU diluted the injectate to 70% PVB and 30% Dolores River fresh water. A geochemical study had predicted that if 100% PVB were injected, it would interact with connate fluids and the dolomitized Leadville Limestone at downhole (initial) temperatures and pressures, and that PVB would then precipitate calcium sulfate, which in turn would lead to restricted permeability (Kharaka, 1997). During October 2001, with the decreased injection rate discussed above, the injectate concentration question was reconsidered. Temperature logging in the injection interval recorded substantial near-wellbore cooling, indicating that if precipitation occurred, it would not be near the wellbore perforations where clogging would be a concern. Further analyses indicated that, if precipitation occurs, its maximum expected rate is ~8 tons of calcium sulfate per day. To put this amount into perspective, injecting at ~230 gpm and assuming a density of 9.86 lbs/gal (17% more dense than fresh water) results in a daily injection mass of ~1633 tons. The maximum expected precipitate is ~0.5% of the daily injection mass.

After considering this new information, the decision was made to begin injecting 100% PVB, in order to increase the amount of salt disposed of with the reduced injection rate initialized in *Phase III.* Injection of 100% PVB began on January 7, 2002, following the December-January 20-day shutdown, and has been maintained since. The same reduced injection rate as in *Phase III*

(230 gpm) and biannual 20-day shutdowns were maintained. The volume of fluid injected during *Phase IV* was 1,110 Mgal (4.2 x 10^9 liters).

Because of the decreased flow rate in *Phase III* and *Phase IV* compared to the earlier phases, the surface pressure remained below the MASIP of 5,000 psi for over decade (mid-2000 to 2011). Hence, there was no need to frequently alter flow rates as was done during *Phases I* and *II*. Because of less frequent injection well shut-ins, the maximum surface and downhole pressures gradually increased during *Phases III* and *IV* (Figure 2-5). In addition, because of the increased density of the 100% PVB injected during *Phase IV* over the 70% PVB : 30% fresh water mix injected previously, the computed downhole pressures increased by ~300 psi immediately following the change to 100% brine in January, 2002.

In response to the increasing surface injection pressures, the injection wellhead equipment was replaced with equipment having a higher pressure rating. Following this equipment upgrade, Reclamation applied to EPA for an increase in the MASIP. EPA granted an increase in the MASIP to 5350 psi when the injection permit was renewed in April, 2004.

2.2.5 Phase V (April 17, 2013 – present)

A M_L 4.4 induced earthquake occurred in the northern Paradox Valley area on January 24, 2013 (Block et al., 2014). In response to this earthquake, injection was halted while a reassessment of the seismic hazard associated with PVU injection was performed. Analyses of the seismic and injection data indicated that the potential for inducing large felt events could likely be reduced by decreasing the long-term average injection pressures (Block and Wood, 2009; Wood et al., 2015). Pressure-flow modeling indicated that reducing the flow rate would reduce wellhead pressures, and forward modeling was used to determine an appropriate flow rate (Wood et al., 2015). In addition, the pressure-flow modeling indicated that changing the injection well shut-in schedule to have shorter, more frequent shut-ins would result in a lower average wellhead pressure, compared to the biannual 20-day shut-ins previously used.

As a result of these analyses, the decision was made in April 2013 to reduce the injection flow rate and increase the frequency of injection well shut-ins. Due to the lag time in obtaining plungers that would allow injection at a lower flow rate, injection was initially resumed on April 17, 2013, maintaining the flow rate at 230 gpm and implementing a 36-hour shut-in every week. On June 6, 2013, following the acquisition of the new plungers, the flow rate was reduced to 200 gpm and the shut-in length was reduced to 18 hours, maintaining the frequency of one shut-in per week. A shut-in duration of 18 hours was chosen so that the total annual shut-in time would be approximately equivalent to that scheduled previously with the biannual 20-day shut-ins. Hence, the nominal flow rate during *Phase V* (200 gpm) was decreased by 13% from that during *Phase IV* (230 gpm), and the total duration of planned shut-ins remained the same.

Because of the frequency of the new shut-in schedule, the durations of any unplanned shut-ins (such as those periodically required for equipment maintenance) are tracked, and those hours are subtracted from the weekly scheduled 18-hour shut-in. The durations of unplanned shut-ins had not been tracked and subtracted from the biannual 20-day shut-ins during earlier injection phases, and hence the total shut-in time during previous years had sometimes varied

substantially, depending on the number and duration of unplanned shut-ins required. Hence, while the nominal flow rate during *Phase V* was decreased by 13% from that during *Phase IV*, the effective decrease in flow rate has been less than this value due to the difference in total shut-in time. The average flow rate during *Phase V* has been 178 gpm, which is ~9% less than the average flow rate of 196 gpm during the previous three years (2010-2012). Through 2015, 253 Mgal (1.0×10^9 liters) of fluid has been injected during this phase.

2.3 Seismic Monitoring

2.3.1 Paradox Valley Seismic Network

During the planning for PVU it was recognized that earthquakes could be induced by the high-pressure, deep-well injection of brine. This was based on comparison to other deep-well injection projects in Colorado, including the Rocky Mountain Arsenal, near Denver, and oil and gas extraction projects near Rangley (Gibbs and others, 1973; Raleigh and others, 1976; Hsieh and Bredehoeft, 1981; Nicholson and Wesson, 1990). In 1983, eight years before the first injection at PVU, Reclamation commissioned a seismic monitoring network to characterize the pre-injection, naturally-occurring seismicity in the Paradox Valley region, and to monitor earthquakes that might be induced once injection operations began. The Paradox Valley Seismic Network (PVSN) was the product of these efforts. Field equipment for an initial 10-station network was acquired and installed in 1983 by the U.S. Geological Survey (USGS), under a Memorandum of Agreement with Reclamation. Nine of these original seismic stations were vertical-component, and the remaining station (PV08) was three-component. For the first six years of monitoring, seismic data from this network were acquired and processed by the USGS at their facilities in Golden, Colorado. In 1990, responsibility for data acquisition and analysis was assumed by Reclamation. The USGS continued to assist Reclamation with the maintenance of the field instrumentation and radio telemetry.

Upgrade and expansion of the original 10-station continuously-telemetered, high-gain seismic network began in 1989. First, a three-component station (PV11) was installed on the mesa just south of the injection well in order to provide better focal depth control and to allow for more sensitive event detection. Three vertical-component stations (PV12-PV14) were also added in 1989 to increase the density of stations surrounding the well. Station PV08 was downgraded in 1989 from a three-component station to a vertical-component only station, because it was determined that the equipment could be better used at the new stations closer to the injection well. Station PV15 was installed in 1995 to replace PV06, which had been vandalized in 1991, 1992, and finally in 1994, when it was abandoned. A second three-component station (PV16) was installed on the mesa north of the injection well in 1999 to further improve near-well coverage.

In October, 2000, a major upgrade to the data telemetry and acquisition was implemented. Up until this time, analog data from all stations had been radio-telemetered through PV08, which then relayed the data stream to Reclamation offices in Montrose, where it was transmitted via microwave and analog telephone links to Denver. In Denver, the analog data from all stations were digitized (using 12-bit digitizers) and processed. In October, 2000, a wide-area network (WAN) link was established at Hopkins Field, near Nucla, and new 16-bit digitizers were

installed there. All analog radio links from the stations were reconfigured to terminate at Hopkins Field, and the use of analog telephone circuits to relay data was discontinued. Station PV08 was no longer used as a radio-telemetry relay. Station PV08 was temporarily removed in October 2003 to accommodate nearby construction activities, and reinstalled in October 2007.

Starting in 2005, upgrades to the high-gain seismic network focused on replacing the analog short-period seismic instrumentation with digital broadband instrumentation. The short-period instrumentation had become obsolete both in terms of the data quality needed for ongoing analyses, and in terms of maintaining equipment that was no longer manufactured. Two key characteristics of the instrumentation constrain data quality: bandwidth and dynamic range. The short-period instrumentation had an effective seismic signal bandwidth of 1-20 Hz. The low end of this range was determined by the natural frequency (1 Hz) of the seismometers used (Geotech model S-13), and the high end by the analog low-pass filter setting (nominally 25 Hz). The bandwidth of the analog stations was insufficient for many analysis purposes, such as accurately identifying complex seismic phases, accurately computing seismic moments of induced earthquakes (which require determination of long-period spectral levels), waveform modeling, or extracting time-domain Green's functions from ambient noise. Furthermore, the effective dynamic range of the analog stations constrained the ratio of the largest to smallest seismic signal that could be recorded on-scale to a factor of only about 1000, which corresponds to approximately two magnitude units. This resulted in seismic signals of earthquakes greater than about M 1.5 being clipped, which limited the use of this important data for magnitude and moment calculations, waveform cross-correlation, and identification of the S-wave arrival. Although 16-bit digitizers (with a dynamic range of 90 dB) were used after 2000, the effective dynamic range of the analog stations remained much less, approximately 10 or 11 bits (60 dB), because of the limited sensitivity of the voltage-controlled oscillators (VCOs) used at the stations to modulate the seismic signals onto the carrier tones used for analog radio telemetry. Modern broadband instrumentation provides much better characteristics, with typical bandwidths of 0.03 to 50 Hz, 24-bit digitizers providing a dynamic range of 135 dB or more, and seismometers typically packaged as a single unit with internal three-component sensors.

In November 2005, the first 3-component broadband seismometer (Guralp model CMG-40TD) was installed at a new station southwest of the injection well (PV17). This instrument uses a 24-bit digitizer integrated within the seismometer case to minimize potential cable noise (digitizers and seismometers separated by a long analog cable can be sensitive to cross-talk at the microvolt level, which is difficult to protect against). Station PV12 was similarly upgraded at about the same time, and stations PV04 and PV14 were converted in May and July of 2007. These first-generation digital stations used digital radios that effectively behaved as a remote RS232 serial data link, and which required the use of "combiner-repeater" (Guralp model CRM-6) modules to combine the serial signals from multiple stations. The first-generation stations exhibited a number of data quality problems, the most severe of which was crosstalk between the GPS antenna cabling (which provided timing for the internal digitizer), and the system providing power to the seismometer (O'Connell, 2008). The crosstalk inherent in the first-generation design resulted in significant spectral spikes in the data at frequencies of 1 Hz and greater, as illustrated in Figure 2-6.

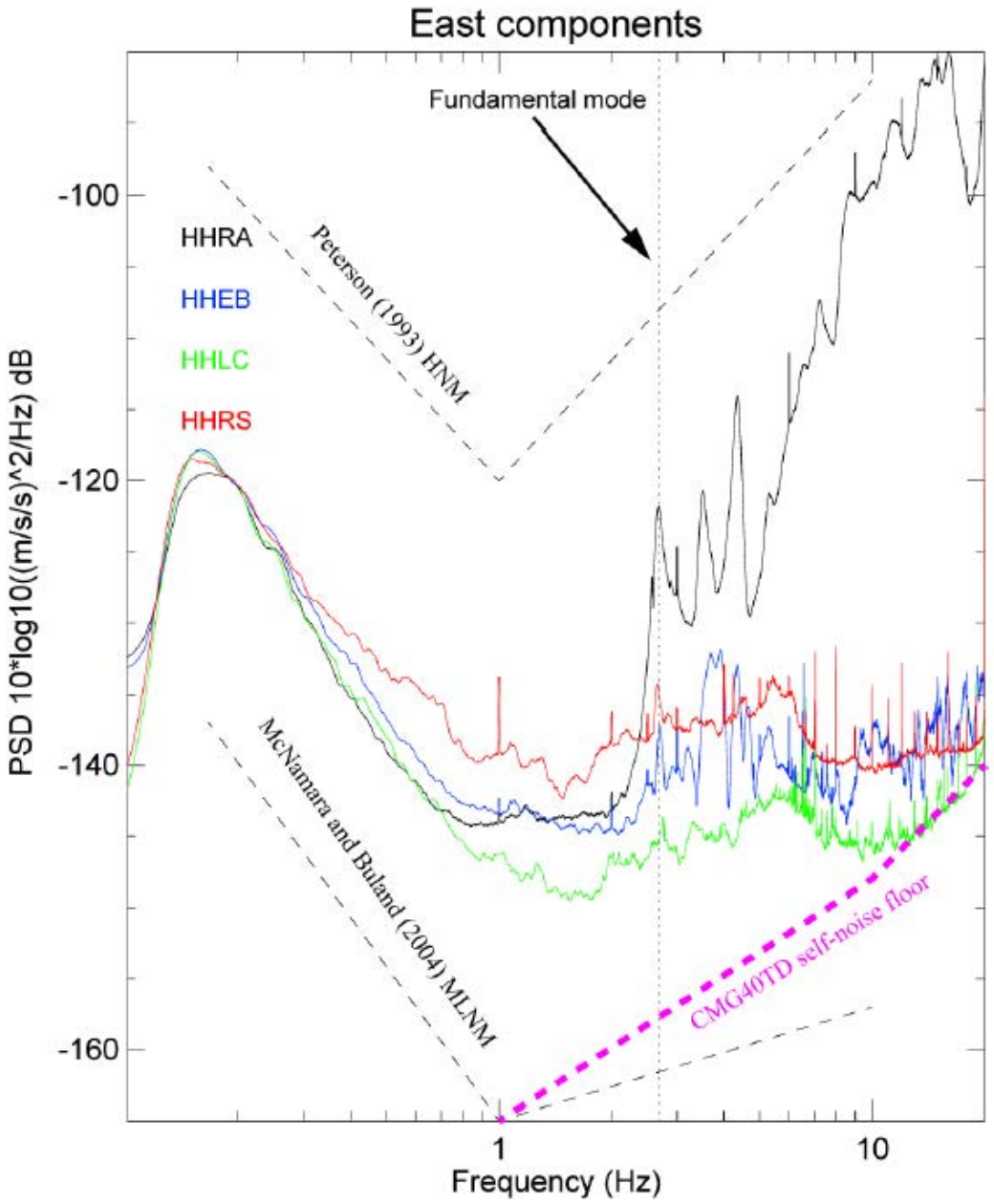

Figure 2-6: Stacked multi-taper acceleration power spectra from the east-west components of Guralp model CMG40TD seismometers installed at four first-generation stations near Hungry Horse Dam, Montana. Windows were 400 seconds in length, and represented ambient conditions (station HHRA was located close to power generation plant at the dam, and therefore exhibited much higher ambient noise levels at frequencies above 2 Hz). The obvious spikes in the spectra at frequencies of 1 Hz and higher were caused by GPS antenna crosstalk problems inherent in the first-generation stations. A new station design was implemented at Paradox Valley to substantially reduce these crosstalk problems. Figure from O'Connell (2008).

A new station design was developed in 2007 and 2008 based on experience from the first generation stations and from similarly-instrumented seismic networks deployed at B.F. Sisk and Hungry Horse Dams (O'Connell, 2008). The new stations incorporated features to minimize the GPS antenna crosstalk problem, as well as to make the system more modular and robust. It

included entirely new seismometer vaults, station enclosures, antennas, solar panels, and Ethernet packet radios. Deployment of the new instrumentation began in 2008, with upgrades of PV02, PV03, PV10, and PV11. In May, 2010 stations PV01, PV05, PV07, PV13, and PV16 were upgraded. In July, 2011, station PV15 was upgraded. In addition, six broadband digital seismic stations (PV18 to PV23) were installed at new sites in 2011. Two of these stations, PV22 and PV23, are replacements for old analog stations PV08 and PV09, respectively. The decision was made to decommission stations PV08 and PV09 because of site conditions resulting in poor seismic data quality. The other four new seismic stations (PV18, PV19, PV20, and PV21) were installed to improve coverage in seismically active areas of interest (including seismicity occurring within 9 km of the injection well and at the northern end of Paradox Valley).

Upgrade of the PVSN seismic stations to broadband digital instrumentation was completed in late 2011. Consequently, Reclamation discontinued maintenance of the obsolete analog seismic stations. Four of those stations went permanently offline during 2011 (PV02, PV07, PV08, and PV15). An additional analog station (PV11) ceased functioning in late 2013. The remaining analog stations were decommissioned in July, 2014, when the data acquisition center at Hopkins Field was moved into a new building.

In addition to the continuously telemetered high-gain seismic array, three event-triggered strong motion instruments were added to PVSN. The first strong motion instrument (station name PVPP) was installed near the injection wellhead in 1997. A second strong-motion instrument was installed near the extraction facilities (PVEF) in 2003, and the third was installed in the nearby community of Paradox, Colorado (PVCC) in 2005. The strong-motion array is designed to measure ground motions from events that are large enough to be felt or cause damage, and which could saturate high-gain array stations closest to the epicenter.

The locations of the PVSN seismograph stations are shown in Figure 2-7. Details about the stations are provided in Table 2-1, including installation date, station type, and number of components. Table 2-2 lists the station location names.

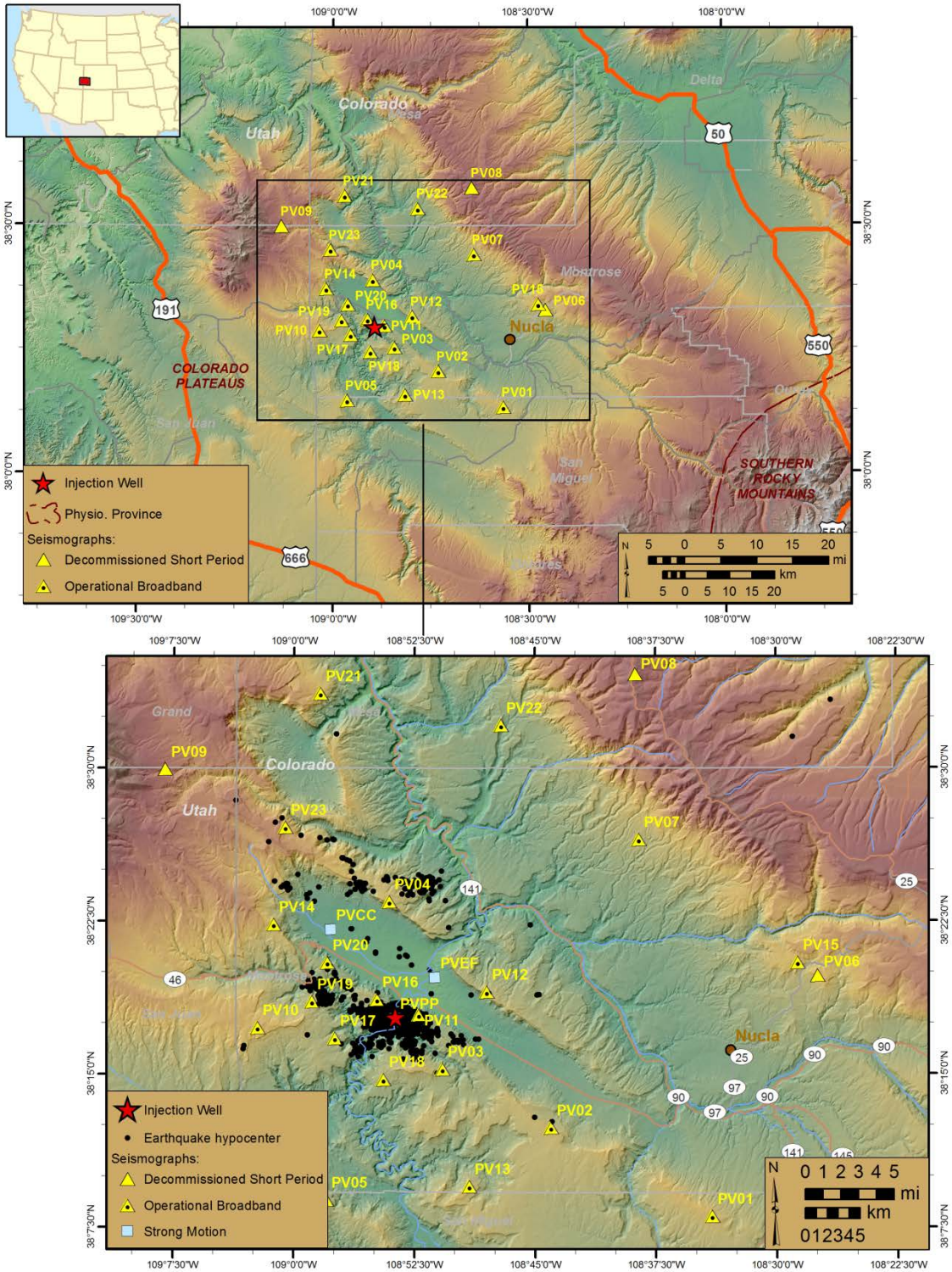

Figure 2-7: Locations of the PVSN seismic stations, PVU injection well, and epicenters of earthquakes less than 8.5 km deep. PVCC, PVEF, & PVPP are the strong motion stations. Station PV06 was replaced by PV15. Physiographic provinces from Fenneman and Johnson (1946).

Table 2-1: PVSN Station Locations and Characteristics

Station Name	Latitude deg., N	Longitude deg., W	Elev. m	Dates of Operation	Station Type	Sensor Direction
PV01	38.13	108.57	2191	5/83-7/16/15 5/10-present	short-period broad-band	vertical triaxial
PV02	38.21	108.74	2177	5/83-8/27/11 10/08-present	short-period broad-band	vertical triaxial
PV03	38.25	108.85	1972	5/83-7/16/15 10/08-present	short-period broad-band	vertical triaxial
PV04	38.39	108.90	2176	5/83-6/06 5/07-present	short-period broad-band	vertical triaxial
PV05	38.15	108.97	2142	5/83-7/16/15 5/10-present	short-period broad-band	vertical triaxial
PV06	38.33	108.46	2243	5/83-8/94	short-period	vertical
PV07	38.44	108.64	2040	6/83-8/27/11 5/10-present	short-period broad-band	vertical triaxial
PV08	38.58	108.65	2950	6/83-9/89 9/89-10/03 10/07-7/12/11	short-period short-period short-period	triaxial vertical triaxial
PV09	38.50	109.13	2662	6/83-7/16/15	short-period	vertical
PV10	38.29	109.04	2266	6/83-7/16/15 10/08-present	short-period broad-band	vertical triaxial
PV11	38.30	108.87	1882	12/89-10/13 10/08-present	short-period broad-band	triaxial triaxial
PV12	38.32	108.80	2092	12/89-7/05 11/05-present	short-period broad-band	vertical triaxial
PV13	38.16	108.82	2158	12/89-7/16/15 5/10-present	short-period broad-band	vertical triaxial
PV14	38.37	109.02	2234	12/89-4/02 6/07-present	short-period broad-band	vertical triaxial
PV15	38.34	108.48	2234	6/95-8/27/11 7/11-present	short-period broad-band	vertical triaxial
PV16	38.31	108.92	2025	7/99-7/16/15 5/10-present	short-period broad-band	vertical triaxial
PV17	38.28	108.96	1991	11/05-present	broad-band	triaxial
PV18	38.25	108.91	1999	7/11-present	broad-band	triaxial
PV19	38.31	108.98	2041	7/11-present	broad-band	triaxial
PV20	38.34	108.97	1852	7/11-present	broad-band	triaxial
PV21	38.56	108.97	2235	7/11-present	broad-band	triaxial
PV22	38.54	108.79	1925	7/11-present	broad-band	triaxial
PV23	38.45	109.01	2456	11/11-present	broad-band	triaxial
PVPP	38.30	108.90	1524	12/97-present	strong motion	triaxial
PVEF	38.33	108.85	1513	10/03-present	strong motion	triaxial
PVCC	38.37	108.96	1617	6/05-present	strong motion	triaxial

Notes: Elevations are relative to mean sea level (msl), the surface elevation of the injection well is 1540 m above msl. Stations with vertical sensor direction are single-component; triaxial are 3-component (vertical, north, and east).

Table 2-2: PVSN Telemetered Sites - Station Location Names

Station	Station Location Name
PV01	The Burn
PV02	Monogram Mesa
PV03	Wild Steer
PV04	Carpenter Flats
PV05	E. Island Mesa
PV07	Long Mesa
PV08	Uncompahgre Butte
PV09	North LaSalle
PV10	Wray Mesa
PV11	Davis Mesa
PV12	Saucer Basin
PV13	Radium Mtn
PV14	Lion Creek
PV15	Pinto Mesa
PV16	Nyswonger Mesa
PV17	Wray Mesa East
PV18	Skein Mesa
PV19	Morning Glory Mine
PV20	W. Nyswonger Mesa
PV21	Cone Mountain
PV22	Blue Mesa
PV23	Carpenter Ridge

2.3.2 Induced Seismicity

Nearly 6,300 relatively shallow (< 8.5 km deep) earthquakes have been recorded in the vicinity of Paradox Valley since injection began in 1991. No shallow earthquakes were detected in six years of seismic monitoring prior to the start of injection operations. The majority of these events have depth estimates between approximately 2.5 and 6.5 km (relative to the ground surface elevation at the injection wellhead), close to the depth of the injection interval (4.3 to 4.8 km). The seismicity has been observed at increasing distance from the injection well over time (Figure 2-8). The initial earthquakes were detected four days after the start of the first injection test in July 1991 and occurred very close to the injection well. As injection continued, earthquakes occurred at progressively increasing radial distances. By 2002, earthquakes were occurring as far as 16 km from the well. The lack of shallow seismicity detected during six years of pre-injection

seismic monitoring, the general correlation of the depths of the earthquakes and the depth of injection, and the spatiotemporal evolution of the seismicity since the start of injection demonstrated in Figure 2-8 strongly suggest that these earthquakes have been induced by PVU fluid injection.

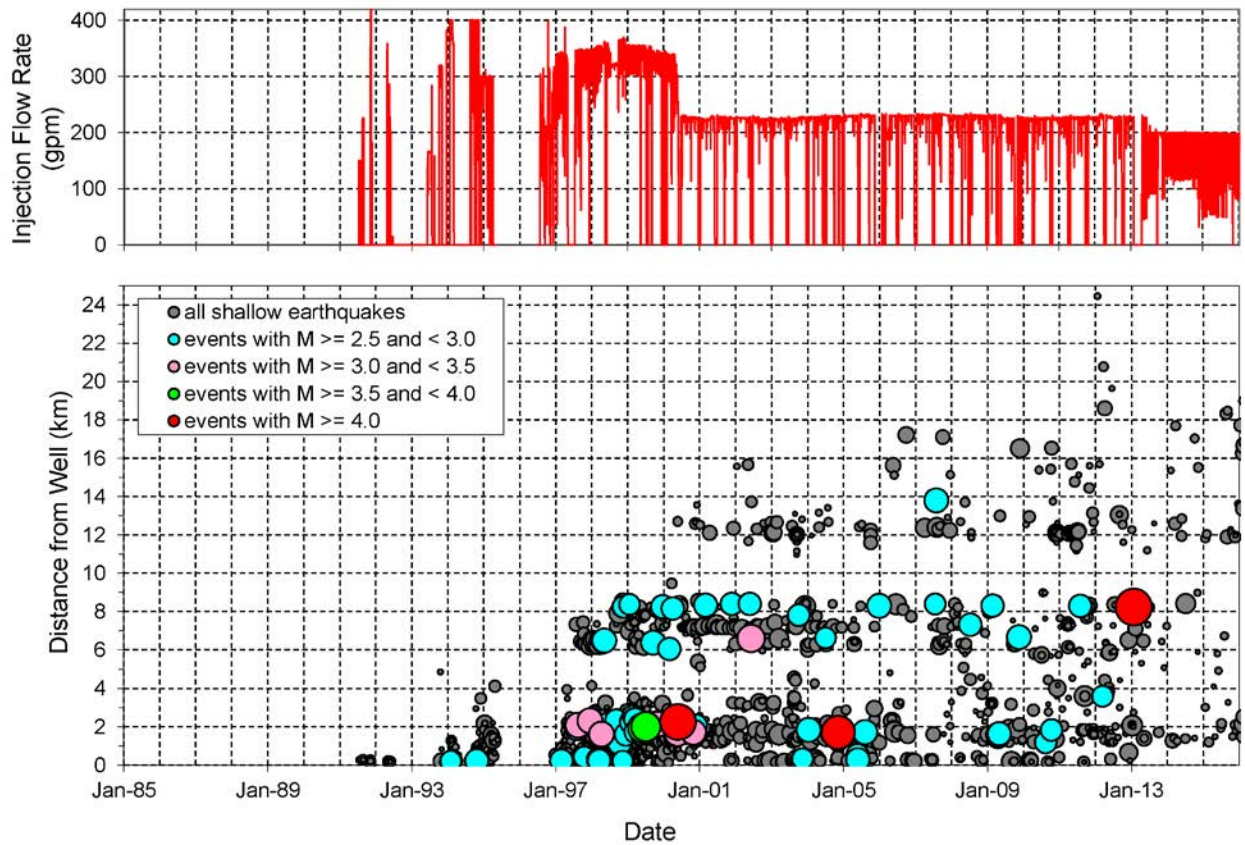

Figure 2-8: Lower plot: scatter plot of earthquakes having magnitude ≥ 0.5 and depth < 8.5 km (relative to the ground surface elevation at the injection wellhead), plotted as a function of date and distance from the PVU injection well. Each circle represents a single earthquake, with the width of the circle scaled by the event magnitude. Upper plot: daily average injection flow rate.

Several distinct groups, or clusters, of induced seismicity have developed over the history of PVU injection operations. By the end of the injection tests in 1995, earthquakes were occurring 3 to 4 km from the well (Figure 2-9a). This area of induced seismicity immediately surrounding the injection well is referred to as the "near-well" region. In 1997, about one year after the start of continuous injection, earthquakes began occurring 6 to 8 km northwest of the injection well (Figure 2-9b). This group of induced seismicity is called the "northwest (NW) cluster". In mid-2000, earthquakes were first detected 12 to 14 km from the injection well, along the northern edge of Paradox Valley (Figure 2-9b). Several distinct clusters of earthquakes have occurred along the northern edges of the valley since 2000 (Figure 2-9c,d). The earthquakes occurring in all of these groups are referred to as "northern valley events". An earthquake was first detected about 6 km southeast of the injection well in 2004 (Figure 2-9c), but the seismicity rate in this area markedly increased beginning in 2010 (Figure 2-9d). This tight group of earthquakes is

referred to as the "southeast (SE) cluster". In recent years, a few isolated earthquakes have been detected in previously aseismic areas, including in the center of Paradox Valley (Figure 2-9d).

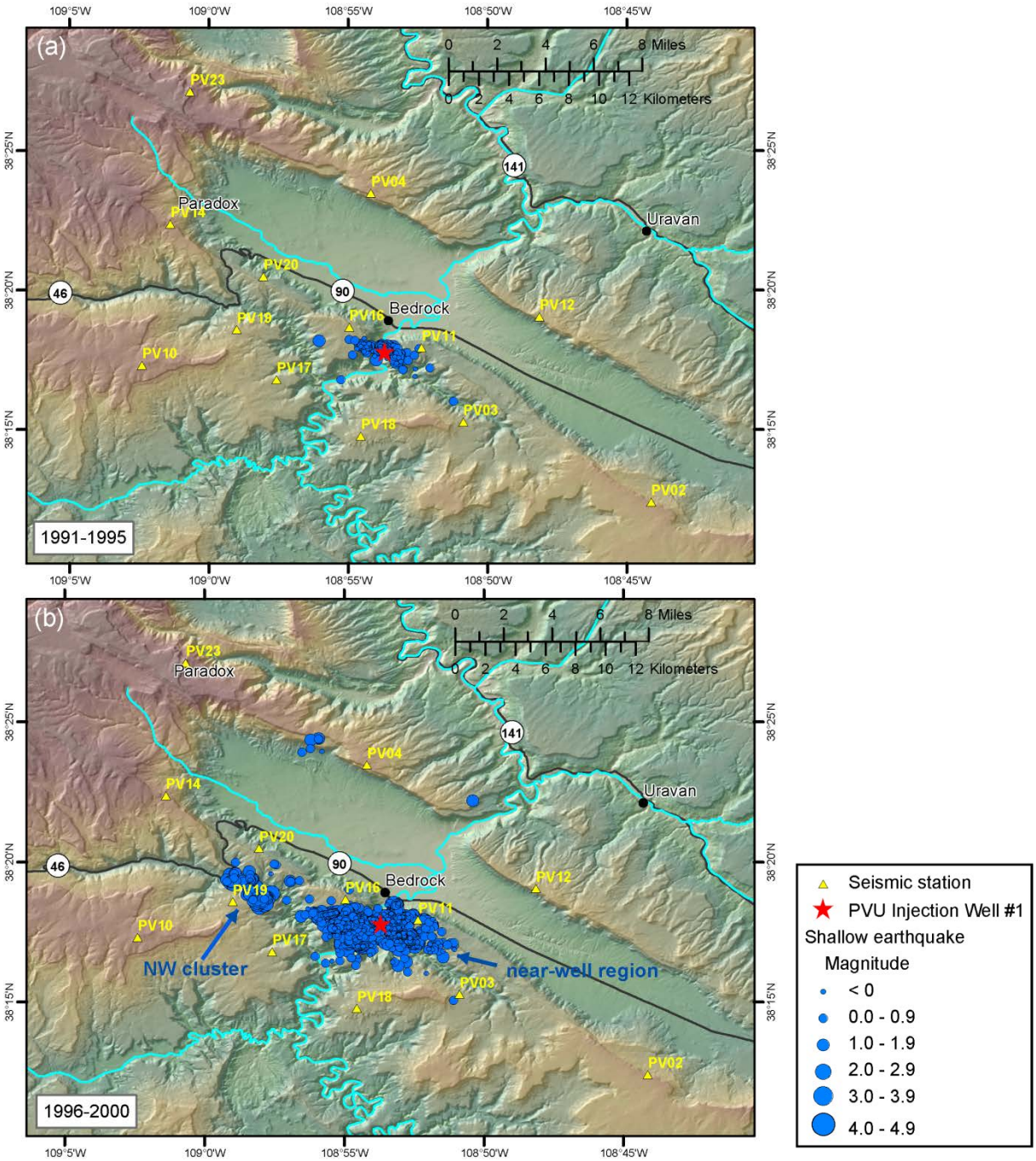

Figure 2-9: Maps showing the spatial distribution of shallow seismicity recorded in the Paradox Valley area over time: (a) injection tests, 1991-1995 (b) continuous injection,1996-2000 (c) continuous injection, 2001-2008 (d) continuous injection, 2009-2015. All earthquakes less than 8.5 km deep (relative to the ground surface elevation at the injection wellhead) are included.

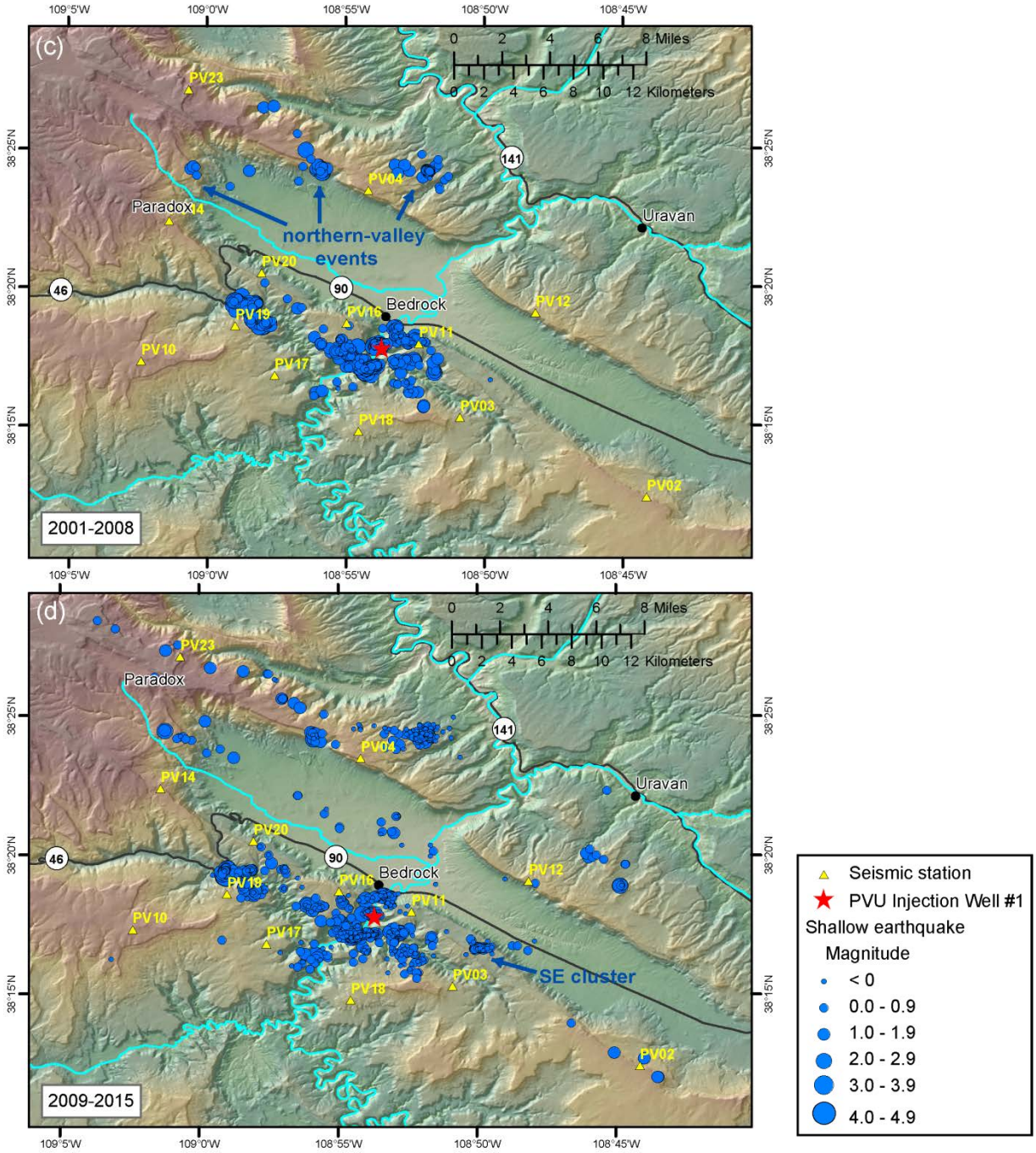

Figure 2-9, continued.

3 Network Operations

3.1 Network Maintenance and Upgrades

One site visit was conducted during 2015. During this visit, two decommissioned analog seismic stations were removed, preventive and remedial maintenance was performed at several digital broadband seismic stations, and lightning protection was installed at several stations. The preventive and remedial station maintenance included replacing batteries, replacing seismometer power supply break-out-boxes (BOBs), replacing or power-cycling GPS BOBs to restore reliable timing, performing vegetation remediation to improve radio communications line-of sight, and raising and re-orienting radio antennas. The data communication hub was also visited; work at the hub included installing additional grounding and replacing/upgrading network switches. Additional details of the work performed during the 2015 site visit are included in the site visit report in Appendix A.

3.2 Network Performance

PVSN network performance depends on the performance of the hardware at individual seismic stations, the robustness of the radio data communications between the stations and the network communication hub at Hopkins Field in Nucla, Colorado, and the reliability of the data acquisition computer systems. The performance of each of these components is discussed below.

Thirteen of the 20 PVSN seismic stations experienced downtimes during 2015 due to hardware or power supply failures, but many were of relatively short duration, lasting only a few days (Table 3-1). Station PV21 was offline for seven and a half months (mid-December, 2014 to July, 2015) due to a hardware failure at the site. Station PV23 experienced intermittent downtimes during the late night hours from mid-December, 2014 until early March, 2015 and then was offline for five months until the end of July. This station began having late night to early morning downtimes again in late December, 2015. Eleven other stations also experienced downtimes beginning in mid to late December. The affected stations include PV01, PV02, PV05, PV07, PV10, PV13, PV14, PV15, PV16, PV21, and PV22 (Table 3-1). The stations went offline during the late night to early morning hours, suggesting that they were caused by an interruption in the power supplies at the stations. The problems at most stations were resolved by December 28. However, station PV22 remained completely offline from December 26 to the time of this report, and station PV23 continued to experience almost nightly downtimes of several hours into spring, 2016. (Additional late night to early morning downtimes also occurred at stations PV02, PV10, PV13, and PV21 during 2016, and station PV21 went offline on March 23, 2016.).

In addition to hardware problems that took stations temporarily offline, the GPS units at three stations malfunctioned in 2015 and caused unreliable timing at these stations for the following periods of time: PV07 from 4/26 to 7/31, PV12 from 8/1 to 8/3, and PV22 from 3/3 to 3/26 and from 6/18 to 8/5. During these times, the stations still provided data for event detection and triggering but the data were not used to compute earthquake locations.

Several stations continue to have degraded radio communications, impacting their ability to continuously transmit seismic data. The stations affected by these problems include PV01, 02, 03, 05, 10, 11, 13, 20, 21, and 22, with the data transmissions from stations PV05 and PV20 being the most severely degraded (Figure 3-1 and Figure 3-2). In such cases, the daily average uptime (the percent of the day that data from the station were transmitted and recorded) is reduced and displays substantial temporal variability (Figure 3-1 and Figure 3-2). The impact of these communication issues for individual stations is small to moderate, reducing the annual station uptime by 1% to 13%. Poor line-of-site radio signal paths may be a contributing factor to the radio telemetry degradation for a few stations. However, the robustness of the radio transmissions declined after the transition to the new communication hub and tower at Hopkins Field in Nucla in July, 2014 and therefore may be at least partially related to an unresolved problem at the hub. Presently, the cause of this problem is under investigation. Considering both the hardware and power supply failures at individual seismic stations and the telemetry data drop-outs, the 2015 annual percent uptime for each station ranged from 40% to 100%, with 14 of the 20 stations having uptimes ≥ 95% (**Error! Reference source not found.**; Table 3-2).

The PVSN data acquisition computer systems were online and functioning well during most of the year. However, there was one relatively long period (12 days) and one short period (6 hours) when the functioning of the data acquisition computer systems was interrupted or substantially degraded. The PVSN network suffered from widespread communication dropouts from February 12 to 24, 2015. During this period, numerous stations lost their IP connections and disconnected from the data acquisition computer system at the PVSN communication hub at Hopkins Field. At various times, up to nine stations lost communication with the data acquisition system simultaneously. Stations that dropped out frequently included PV01, PV02, PV05, PV13, PV20, PV22, and PV23. During this period, Reclamation staff monitored the data acquisition system almost continuously and manually re-connected station communications every few hours. This condition lasted for 12 days until the cause of the problem was successfully diagnosed. The problem was resolved on February 24 with re-installation of the Windows 2008 server network interface card (NIC) driver. The only time during 2015 when PVSN was completely offline occurred on August 27 and lasted only 6 hours. The data acquisition computer systems were offline from approximately 8:15 to 14:07 (UTC), due to a power failure at Hopkins Field. Unfortunately, the generator that was designed to provide back-up power in such circumstances also failed. The generator was repaired in September.

We have been computing and tracking the annual percent uptime of PVSN since 2000. These annual uptimes can be used to compute seismicity rates that are corrected by the number of days that the network was functioning. In 2015, PVSN was only completely offline for six hours (in August). However, event detection was likely impacted during the 12 days in February when up to nine stations were disconnected from the network simultaneously and during the 5 days in December when 8 to 12 stations were offline simultaneously. Considering the six hours that PVSN was offline in August and giving a 50% rating for the days in February and December when multiple stations were offline simultaneously yields an annual PVSN uptime of 97.6%. This value is comparable to the annual PVSN uptimes achieved since 2008 (Table 3-4).

3.3 Data Acquisition Software Transition Testing

Work was performed during 2015 to test a potential upgrade of the computer software that is used for PVSN data acquisition. This software package, called *Earthworm*, was originally developed by the USGS in the 1990s and is still widely used in the seismological community (Johnson and others, 1995; Earle and others, 2003; Friberg and others, 2010). The original *Earthworm* software used by Reclamation was developed directly from the USGS version, which only supported computers running either the Solaris or Windows NT operating systems and did not support the POSIX-compliant system calls used by most other UNIX-based operating systems of that era. In 2000, Reclamation modified the USGS *Earthworm* code to use the POSIX system calls, which allowed it to run on the SGI IRIX and HP versions of UNIX, and to fix many low-level hardware dependencies. Reclamation's POSIX version of *Earthworm* was provided to the open-source community in 2002 and eventually evolved into the version currently running under the Linux operating system, which is also POSIX-based. Reclamation continued to develop and operate its internal version of the *Earthworm* code and added customizations and bug fixes. To take advantage of new features available only in the current open-source *Earthworm* software, which is supported by a private company and an *Earthworm* community forum, work was performed in 2015 to explore the transition from Reclamation's in-house version to the current open-source version.

To understand whether this transition would cause any changes in PVSN's event detection capabilities, event triggers from both versions running simultaneously were compared for several weeks. Initial testing indicated differences in event detection. Detailed comparisons of the event triggering on the two systems indicated that neither version of the software was performing the event detection correctly all of the time. The cause of this problem, and its resolution and effect on PVSN's event detection capabilities, is explained in detail in Appendix B. The problem was resolved on May 1, 2015, by changing the value of a critical parameter in one of *Earthworm's* configuration files. Following this adjustment, side-by-side comparison of the event triggers from the two versions of *Earthworm* was performed for three months (May – July, 2015). Detection of local earthquakes of interest was improved and found to be identical using both software versions.

Following the testing of the open-source version of *Earthworm*, a decision was made to transition PVSN's data acquisition software to the open-source version in 2016, when the existing PVSN data processing software is also transitioned to new computer systems. This process was deemed to be the most efficient way to make the changes in both the data acquisition and data processing computer systems that are needed to meet new security requirements, while at the same time minimizing disruption to PVSN's real-time data processing capabilities. The transition is ongoing and is expected to be completed in 2016.

Table 3-1: Performance of PVSN seismic stations during 2015

Station	Performance
PV01	Experienced an early morning downtime on 12/26/15, likely due to a lack of power. Otherwise online and functioning normally.
PV02	Experienced late night to early morning downtimes from 12/13/15 to 12/28/15, likely due to a lack of power. Otherwise online and functioning normally.
PV03	Online and functioning normally throughout the year.
PV04	Online and functioning normally throughout the year.
PV05	Experienced an early morning downtime on 12/26/15, likely due to a lack of power. Otherwise online and functioning normally.
PV07	The GPS clock was not providing reliable timing from 4/26/15 to 7/31/15. Experienced late night to early morning downtimes from 12/24/15 to 12/27/15 (including being offline from 12/24/15 17:49 to 12/26/15 10:49 local time), likely due to a lack of power. Otherwise online and functioning normally.
PV10	Experienced late night to early morning downtimes from 12/25/15 to 12/27/15, likely due to a lack of power. Otherwise online and functioning.
PV11	Online and functioning normally throughout the year.
PV12	The GPS clock was not providing reliable timing from 8/1/15 to 8/3/15. Otherwise online and functioning normally.
PV13	Experienced late night to early morning downtimes from 12/16/15 to 12/28/15 (including being offline from 12/23/15 23:04 to 12/26/15 11:49 local time), likely due to a lack of power. Otherwise online and functioning normally.
PV14	Offline from 12/25/15 21:04 to 12/28/15 11:04 (local time), likely due to a lack of power. Otherwise online and functioning normally.
PV15	Offline from 12/24/15 0:04 to 12/28/15 11:34 (local time), likely due to a lack of power. Otherwise online and functioning normally.
PV16	Offline from 12/25/15 23:34 to 12/27/15 10:49 (local time), likely due to a lack of power. Otherwise online and functioning normally.
PV17	Online and functioning normally throughout the year.
PV18	Online and functioning normally throughout the year.
PV19	Online and functioning normally throughout the year.
PV20	Online and functioning normally throughout the year.
PV21	The station was offline from 12/14/14 until 7/29/15 due a hardware failure at the station. Experienced late night to early morning downtimes from 12/26/15 to 12/27/15, likely due to a lack of power.
PV22	The GPS clock was not providing reliable timing from 3/3/15 to 3/26/15 and 6/18/15 to 8/5/15. Station went offline on 12/26/15.
PV23	Station began having late night to early morning downtimes in mid-December, 2014. Station was offline from 3/3/15 until 7/30/15, due to a hardware failure at the station. Experiencing late night to early morning downtimes since 12/24/15.

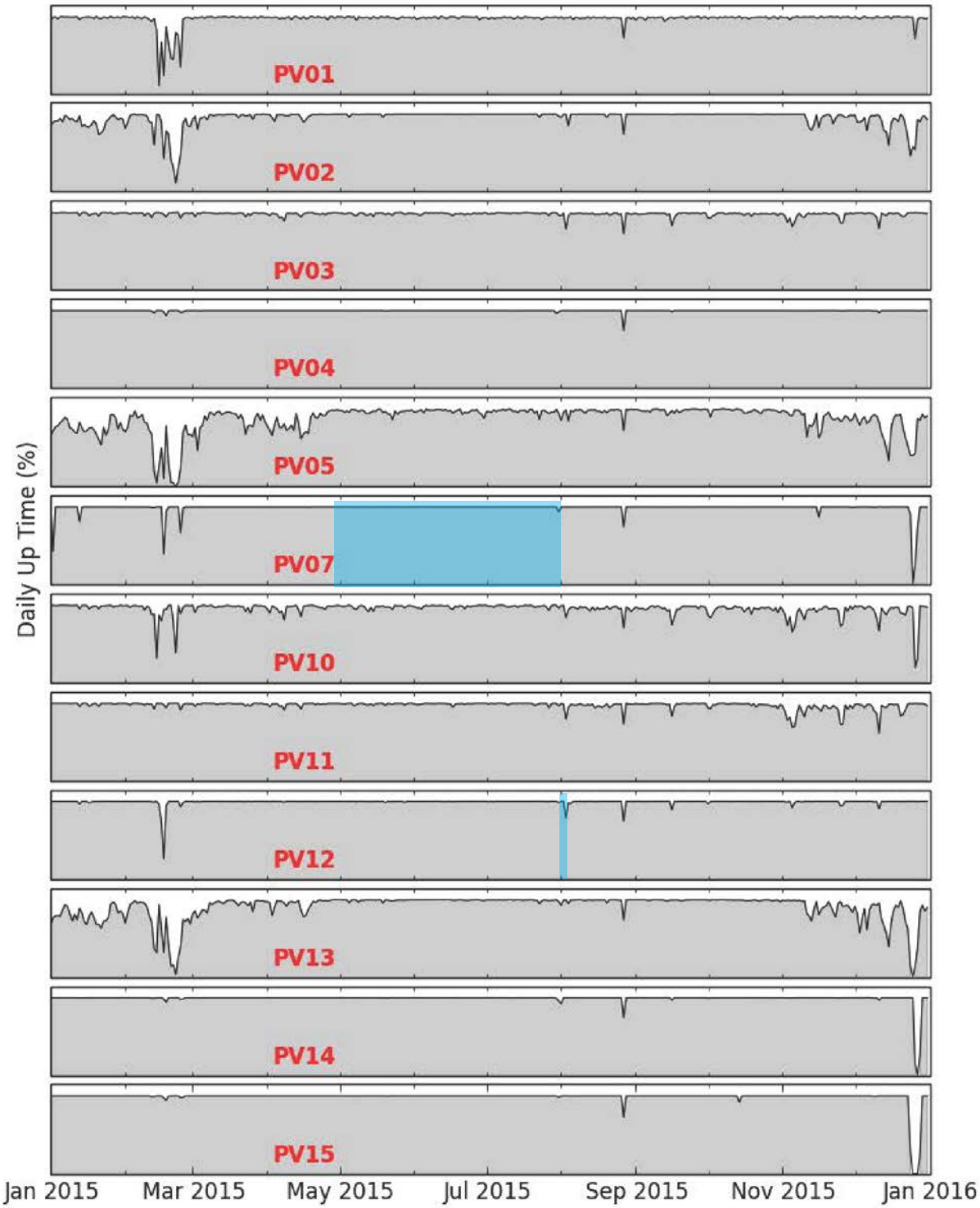

Figure 3-1: Daily uptime (%) for each PVSN seismic station during 2015. Vertical axes on plots are scaled from 0 to 115%. Filled gray areas represent daily uptime, while dips in the filled volume show decreases in uptime. A long period of zero uptime at a single station is the result of a hardware failure at that station. Daily variance in uptime that is uncorrelated between stations is generally the result of poor radio communications with a given station. Correlated decreases in uptime are usually the result of failures in the data acquisition computer systems; the correlated decrease in uptime in late December is due to simultaneous power failures at multiple stations. Shaded blue areas indicate unreliable station timing.

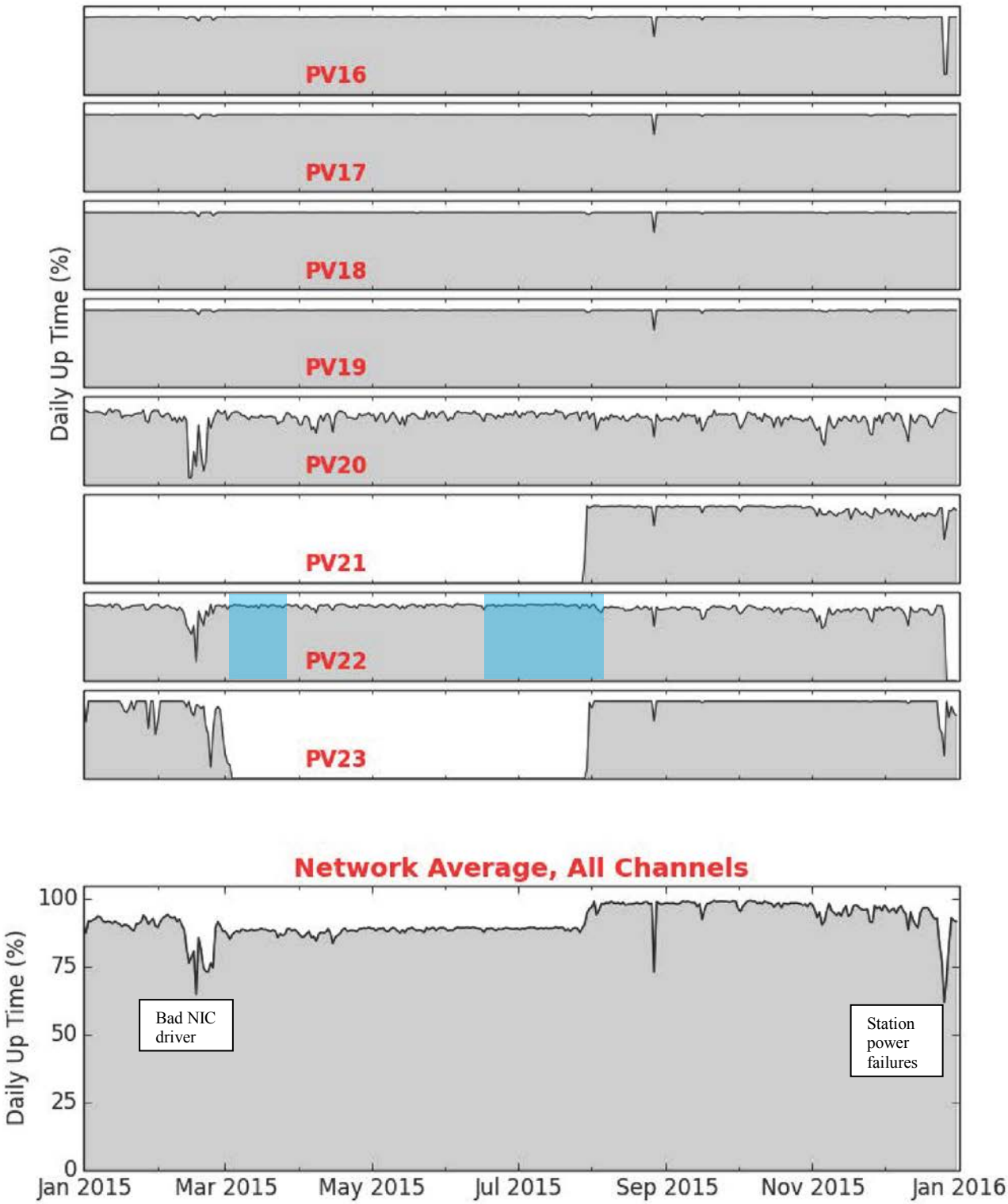

Figure 3-2: Same as Figure 3-1 for the rest of the PVSN stations. Bottom plot shows the daily average performance for all PVSN stations.

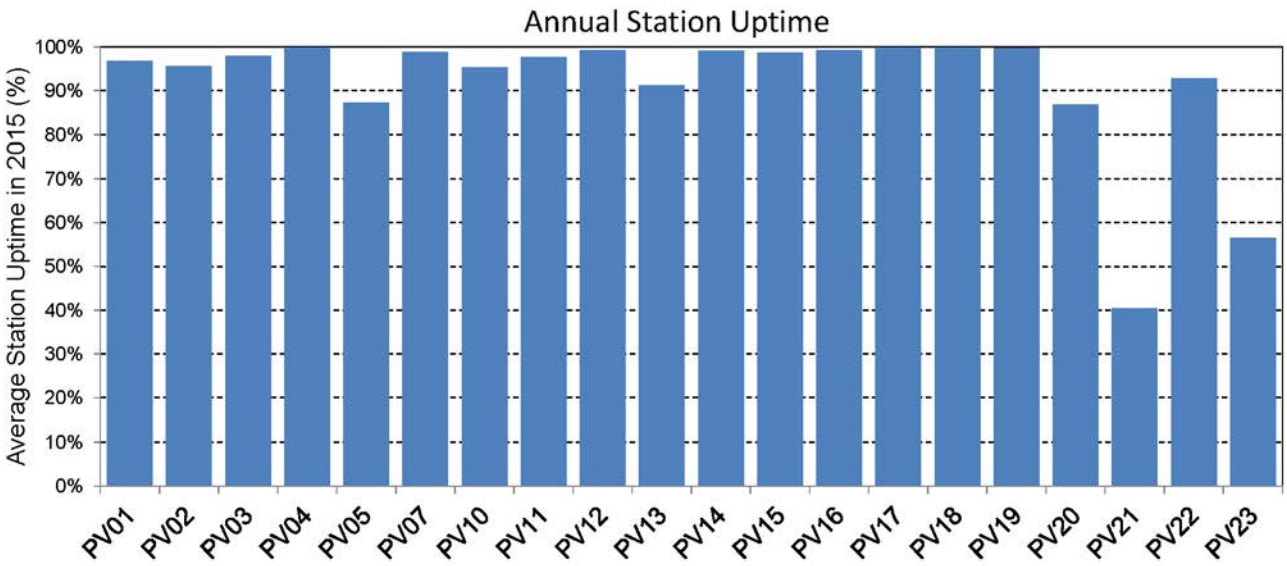

Figure 3-3. Graph of annual (2015) uptime for each PVSN seismic station.

Table 3-2: PVSN station uptime in 2015.

Station	Annual Station Uptime in 2015
PV01	97%
PV02	96%
PV03	98%
PV04	100%
PV05	87%
PV07	99%
PV10	95%
PV11	98%
PV12	99%
PV13	91%
PV14	99%
PV15	99%
PV16	99%
PV17	100%
PV18	100%
PV19	100%
PV20	87%
PV21	40%
PV22	93%
PV23	56%

Table 3-3: Times when PVSN data acquisition was down or degraded in 2015

Down Period (UTC)	Reason
2/12 – 2/24	Problematic network interface card (NIC) driver on data acquisition computer caused data communications to be repeatedly lost for up to 9 stations at a time
8/27 8:15 to 14:07	Acquisition systems down due to power failure at the communication hub at Hopkins Field in Nucla, Colorado and subsequent failure of the generator power backup system
12/24 – 12/28	Up to 12 stations were offline simultaneously, likely due to power supply problems at the stations

Table 3-4: Annual PVSN data acquisition uptime

Year	Annual Number of Down Days	Percent Uptime
2000	24	93.4%
2001*	**	**
2002	5	98.6%
2003	14.5	96.0%
2004	16	95.6%
2005	34	90.7%
2006	47	87.1%
2007	37	89.9%
2008	10	97.2%
2009	6.5	98.2%
2010	0	100%
2011	12.2	96.7%
2012	2.2	99.4%
2013	4.6	98.8%
2014[1]	10.3	97.2%
2015[2]	8.7	97.6%

**not tabulated in 2001

[1] includes 40.5 hours of downtime in September 2014 when network was operating but event detection was severely degraded due to malfunctioning of data acquisition software

[2] includes 50% rating for 12 days in February and 5 days in December when network was operating but monitoring was substantially degraded due to absence of data from 8-12 stations simultaneously.

4 Seismic Data Recorded in 2015

4.1 Annual Summary

One hundred and thirty-three earthquakes were recorded within or near the perimeter of PVSN during 2015. The map in Figure 4-1 shows the epicenters of these events (colored circles), as well as the epicenters of all earthquakes recorded in previous years (gray circles). During 2015, 77 earthquakes were detected in the near-well region of induced seismicity (within 5 km of the injection well, red circles in Figure 4-1), four earthquakes were detected in the northwest (NW) cluster (6 to 9 km northwest of well, blue circles), six earthquakes were detected in the southeast (SE) cluster (6 to 7 km southeast of well, green circles), and 23 earthquakes were detected in areas of recurring seismicity around the northern edge of Paradox Valley (yellow circles). In addition, seven earthquakes occurred beneath north-central Paradox valley, in areas that have been seismically active since 2010 (orange circles in Figure 4-1; four of the events occurred at the same location). The remaining 16 earthquakes occurred in areas that have experienced little to no previous seismic activity. Fifteen of these events have depths less than 7 km (relative to the ground surface elevation at the injection well) and are inferred to be induced (white circles in Figure 4-1). Two of these 15 shallow events (nearly co-located) occurred 18 km southeast of the injection well, close to seismic station PV02. Events were first detected in this area in late 2014. Both of the events recorded in 2015 occurred at a depth of 5.6 km, which is consistent with the depths of the two events detected in 2014. An additional shallow event occurred 12.5 km southeast of the injection well; its estimated depth is 4.7 km. Three events occurred in south-central Paradox Valley, at depths ranging from 4.2 km to 6.5 km. Nine shallow events occurred in a cluster approximately 3.5 to 5.2 km east-northeast of seismic station PV12. The depths of these events range from 5.2 km to 6.9 km. The remaining earthquake recorded during 2015 occurred 18.9 km northeast of the injection well and has an estimated depth of 10.3 km (purple circle in Figure 4-1). Because of this event's depth, distance from the injection well, and distance from shallow, likely-induced earthquakes, we tentatively consider this earthquake to be naturally-occurring.

The numbers and magnitudes of the earthquakes recorded during 2015 in each of the location categories are summarized in Table 4-1. The date and time of occurrence, latitude, longitude, elevation, depth, and computed duration magnitude of each earthquake are listed in Appendix C. The largest earthquake recorded in 2015 that is interpreted as being induced by PVU injection has a duration magnitude (M_D) of 1.6 and occurred in the new seismicity cluster east of station PV12.

Because of the increasing number of shallow, likely-induced earthquakes occurring in previously aseismic areas, and because the seismicity is becoming more dispersed rather than strictly occurring within distinct clusters, we are introducing a new protocol for classifying the observed seismicity. Under this new scheme, the earthquakes are classified into four categories based on their depths (relative to the ground surface elevation at the injection well, 1.524 km) and distances from the injection well:

1. Shallow near-well: depth ≤ 10 km, distance from injection well ≤ 5 km
2. Shallow intermediate: depth ≤ 10 km, distance from injection well > 5 km and ≤ 10 km
3. Shallow distant: depth ≤ 10 km, distance from injection well >10 km
4. Deep: depth > 10 km, any distance from injection well

The earthquakes recorded during 2015 are color-coded using this revised classification scheme in the map presented in Figure 4-2. By comparing this map with the previous one (Figure 4-1), we can see that events in the near-well seismicity cluster generally fall within the new "shallow near-well" category. Events in the NW and SE clusters and most events occurring within Paradox Valley fall within the "shallow intermediate" category. The northern-valley seismicity clusters and the recent seismicity occurring near stations PV02 and PV12 fall within the "shallow distant" category. The numbers and magnitudes of the earthquakes recorded during 2015 in each of the new location categories are summarized in Table 4-2.

The local earthquakes recorded by PVSN during 2015 are plotted as a function of date, earthquake magnitude, and old location category in Figure 4-3. The same type of graph using the new location categories is presented in Figure 4-4. These graphs show a general increase in the rate of occurrence of near-well events beginning in April, 2015 and an increase in the rate of northern-valley and other shallow distant events beginning in July.

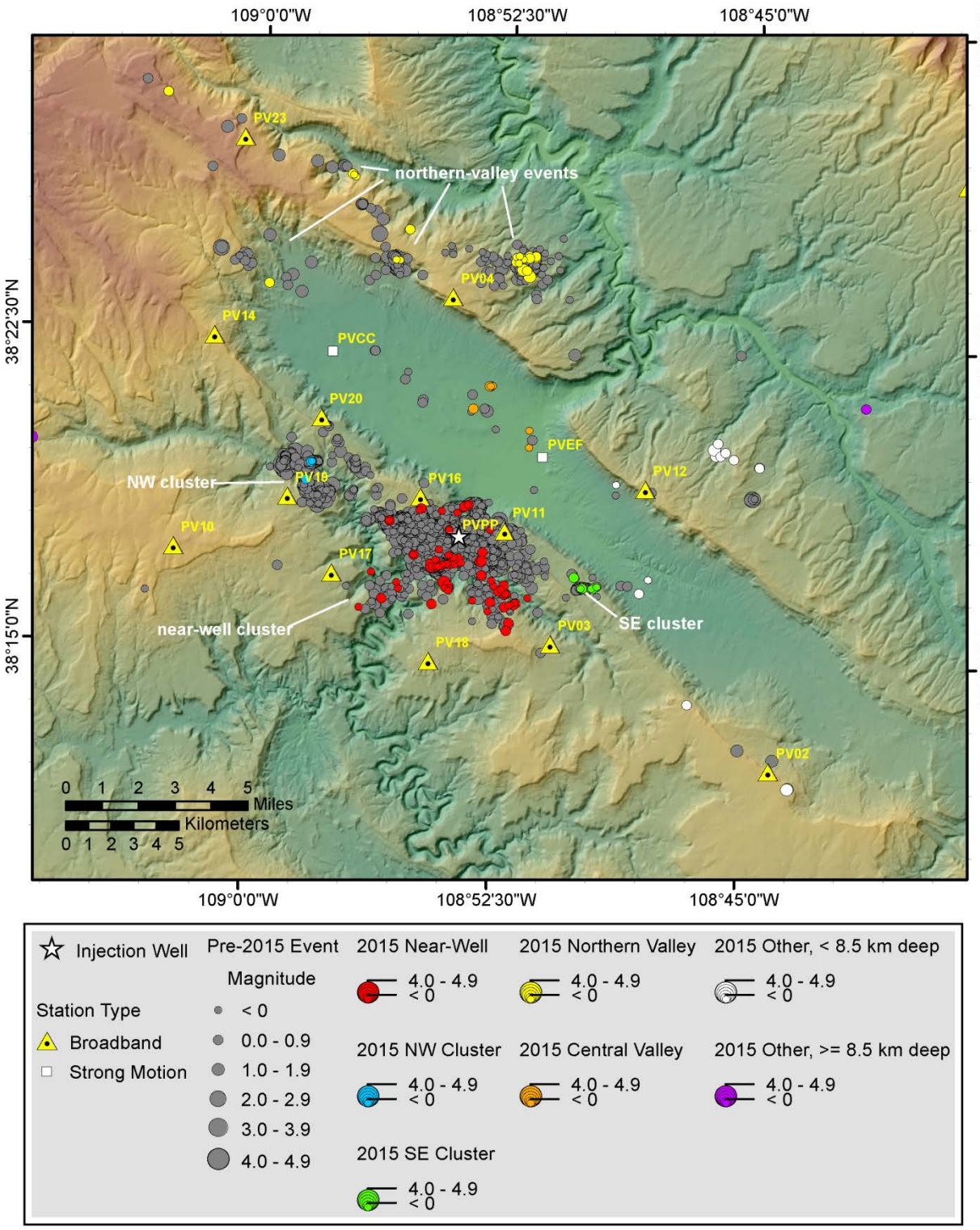

Figure 4-1: Locations of local earthquakes recorded by PVSN during 2015 (colored circles) and previous years (gray circles). The events that occurred during 2015 are color-coded using the old event location categories.

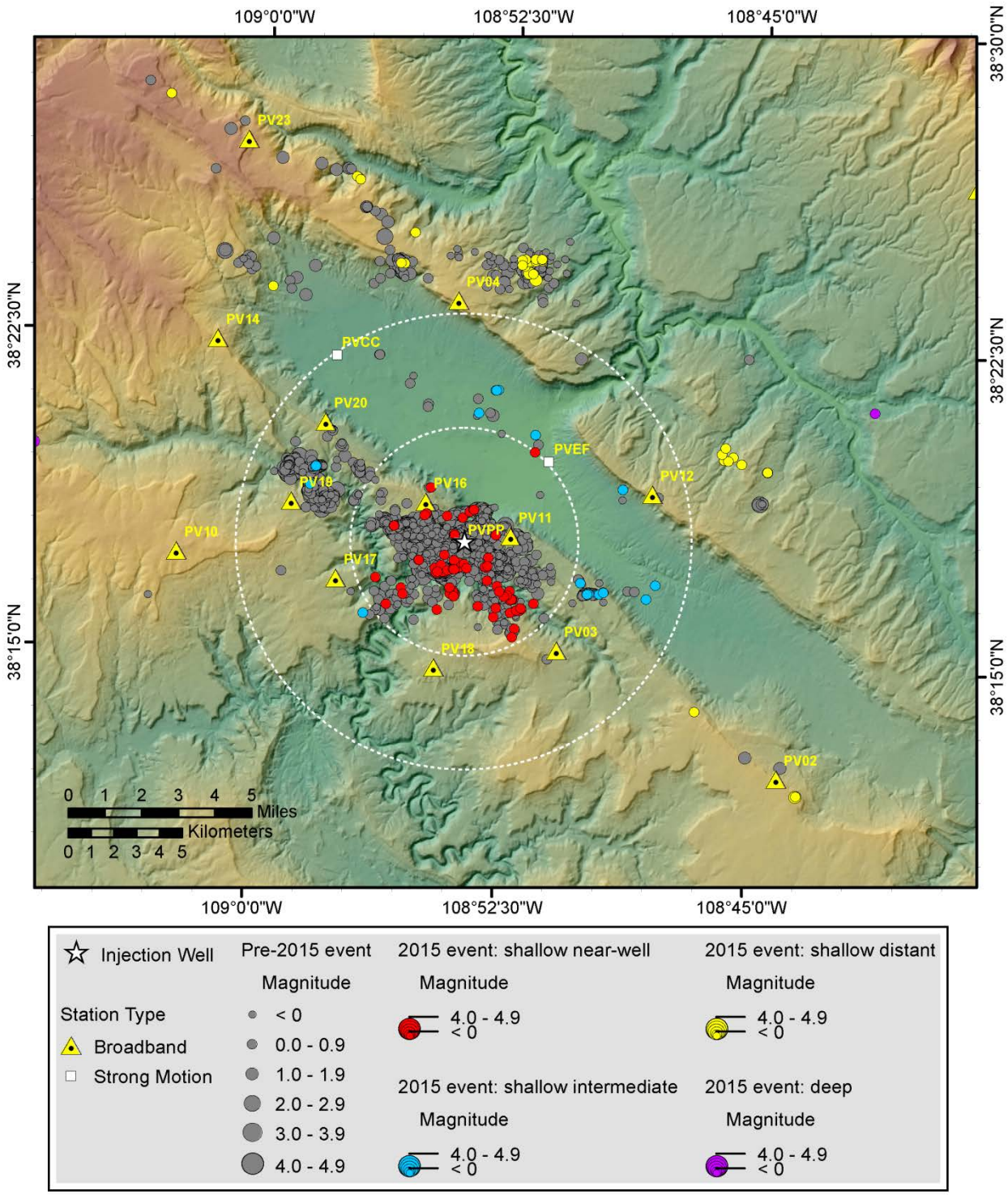

Figure 4-2: Locations of local earthquakes recorded by PVSN during 2015 (colored circles) and previous years (gray circles). The events that occurred during 2015 are color-coded using the new event location categories.

Table 4-1: Summary of events recorded during 2015 by old event location categories

Location Category	Number of Earthquakes Recorded	Number of Earthquakes with $M_D \geq 0.5$	Magnitude Range
near-well	77	10	-1.1 – 1.1
NW cluster	4	0	-0.5 – 0.3
SE cluster	6	1	-0.3 – 0.7
north-central valley	7	2	-0.5 – 0.9
northern valley	23	4	-0.9 – 1.0
other	16	7	-0.5 – 1.6
TOTAL	133	24	-1.1 – 1.6

Table 4-2: Summary of events recorded during 2015 by new event location categories

Location Category	Depth	Distance from well	Number of Earthquakes Recorded	Number of Earthquakes with $M_D \geq 0.5$	Magnitude Range
shallow near-well	≤ 10 km	0 to 5 km	77	10	-1.1 – 1.1
shallow intermediate		>5 to 10 km	20	3	-0.5 – 0.9
shallow distant		>10 km	35	10	-0.9 – 1.6
deep	>10 km	all distances, within perimeter of PVSN	1	1	0.9
		TOTAL	133	24	-1.1 – 1.6

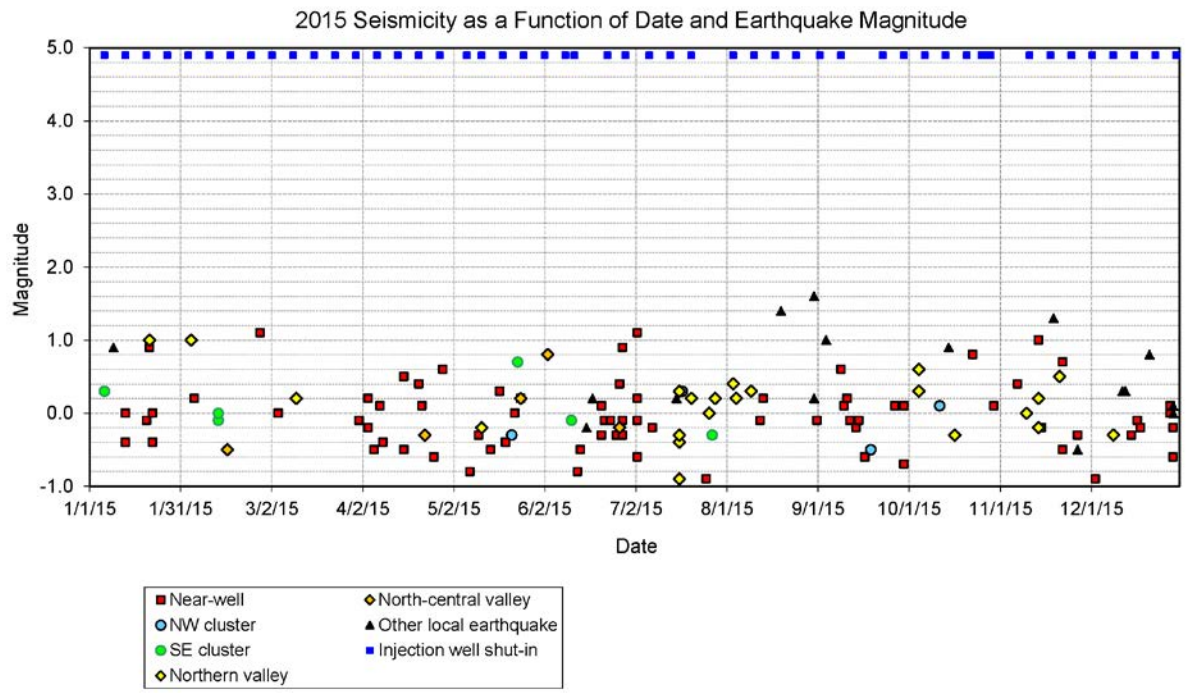

Figure 4-3: Earthquakes recorded by PVSN during 2015, plotted as a function of date, magnitude, and old event location categories. The dates of injection well shut-ins are indicated at the top of the graph.

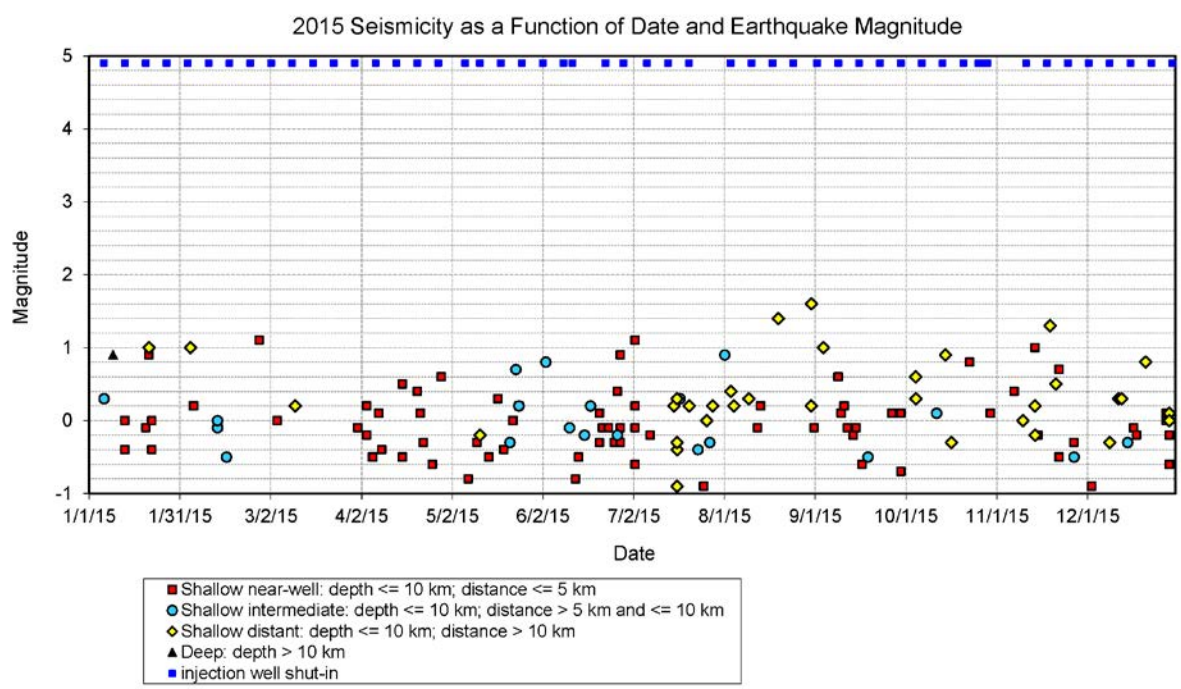

Figure 4-4: Earthquakes recorded by PVSN during 2015, plotted as a function of date, magnitude, and new event location categories. The dates of injection well shut-ins are indicated at the top of the graph.

4.2 Shallow Earthquakes within 10 km of the Injection Well

4.2.1 2015 Seismicity

The hypocenters of the earthquakes that occurred in 2015 within 10 km of the injection well are compared to those from previous years in the map in Figure 4-5 and in the vertical cross sections presented in Figure 4-6. In these figures, the earthquakes that occurred during 2015 and those that occurred in previous years are each separated into two categories based on how precise the computed hypocenters are relative to the other events. The best earthquake locations were computed using a relative earthquake location method employing precise arrival time differences between pairs of earthquakes (computed using waveform cross-correlation). The poorer earthquake locations were computed using an algorithm employing manually-determined absolute arrival times, because the waveform data were not of sufficient quantity or quality to include these events in the relative location. As seen in the map and cross sections, the earthquakes induced within 10 km of the injection well during 2015 mostly occurred in areas of previous seismic activity. Much of the seismicity in 2015 occurred south of the injection well, at distances between approximately 1 and 5 km (Figure 4-5).

Ten shallow, likely-induced earthquakes occurred beneath Paradox Valley in 2015. Seven of these occurred in the northern part of the valley (north of seismic station PVEF), an area where several events have been detected each year since 2010. The other three occurred in the more southern part of the valley, where little previous seismicity has been observed. The depths of these ten events range from 4.2 km to 6.9 km, and their magnitudes range from M_D -0.5 to M_D 0.9.

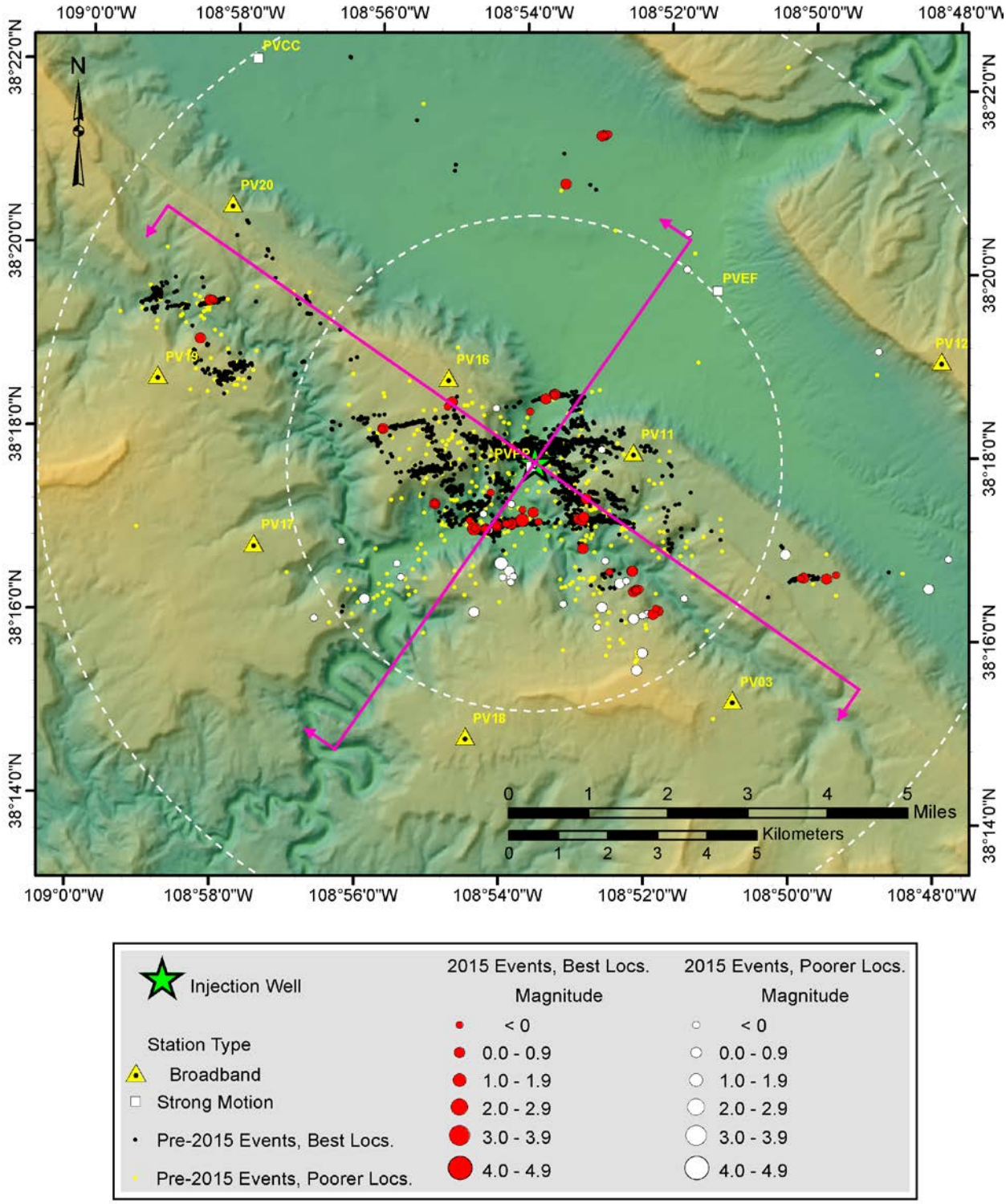

Figure 4-5: Map showing the epicenters of shallow earthquakes (< 8.5 km depth) in the vicinity of the injection well in 2015, compared to the locations of previously-induced events. The white dashed circles indicate radial distances of 5 and 10 km from the injection well. The magenta lines indicate the orientations of the cross sections presented in Figure 4-6.

(a) Cross section parallel to Paradox Valley, looking to the southwest

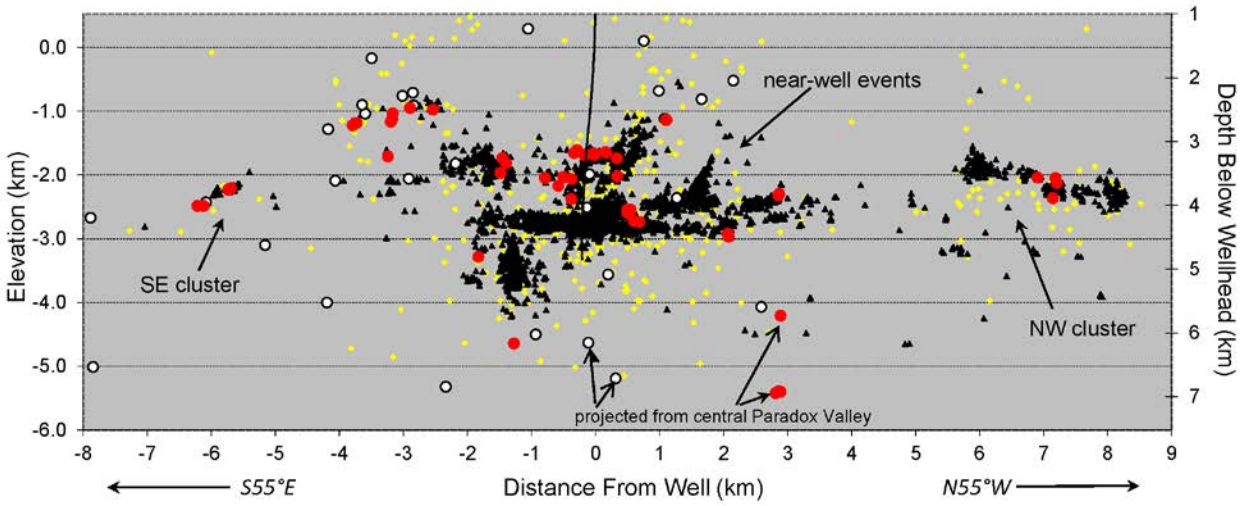

(b) Cross section perpendicular to Paradox Valley, looking to the northwest

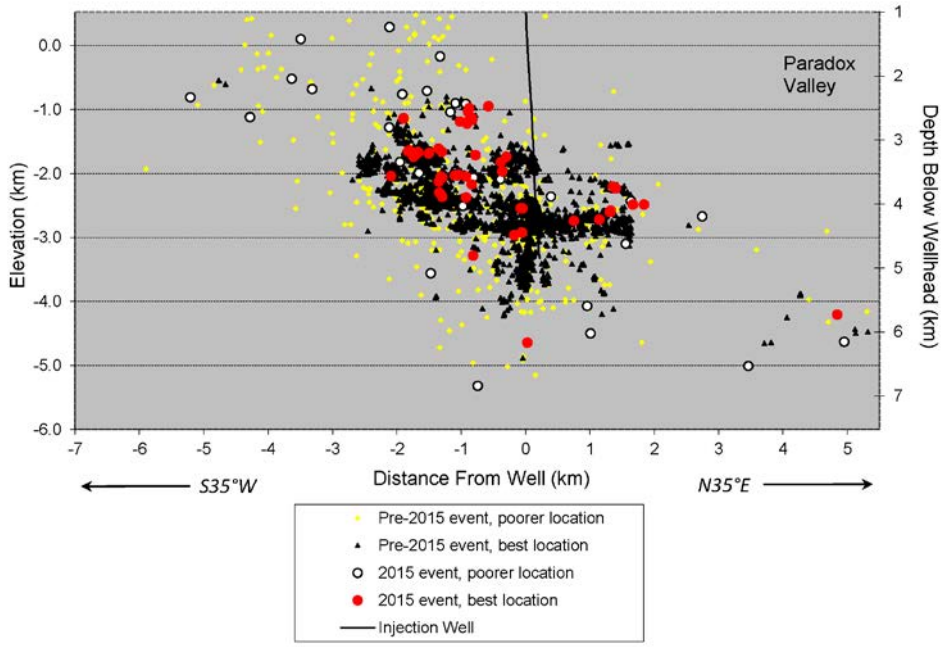

Figure 4-6: Vertical cross sections showing the hypocenters of earthquakes occurring within approximately 10 km of the injection well in 2015, compared to the locations of previously-induced events: (a) section parallel to Paradox Valley (b) section perpendicular to Paradox Valley. The orientations of the cross sections are indicated by the magenta lines in Figure 4-5.

4.2.2 Comparison to 2014 Seismicity

The number of earthquakes observed within 10 km of the injection well increased by 143% in 2015 (97 events) compared to 2014 (40 events). However, much of this change is due to an improvement in PVSN's event detection capabilities, which is described in Appendix B. When considering only events with M_D 0.5 or larger, which was the approximate completeness threshold during 2014, the change is much smaller. Thirteen events with $M_D \geq 0.5$ were detected within 10 km of the injection well in 2015, compared to 10 such events in 2014, an increase of 30%.

The numbers of earthquakes recorded during 2015 and 2014 are plotted as a function of magnitude in Figure 4-7. Individual histograms are shown for earthquakes within 5 km of the injection well, for those at distances of 5 to 10 km from the well, and for all events within 10 km of the well. (These radial distances are indicated by the white dashed circles on the map in Figure 4-5.) As discussed above, most of the differences in event counts between the two years occurs for magnitudes below M_D 0.5 and are largely due to changes in PVSN's event detection capabilities. In both the near-well region (0 – 5 km from the well) and the intermediate region (5 – 10 km from the well), the number of events between M_D 0.5 and M_D 1.0 increased from 2014 to 2015, while the number of events with $M_D > 1.5$ decreased. However, the absolute numbers of events in these magnitude ranges recorded during both years are small and therefore the statistics are not very robust. The largest earthquake recorded during 2014 within 5 km of the injection well had a magnitude of M_D 1.7. The largest earthquake within 5 km of the well recorded during 2015 had a smaller magnitude, M_D 1.1. The maximum earthquake magnitude in the 5-10 km distance range decreased from M_D 2.3 in 2014 to M_D 0.9 in 2015.

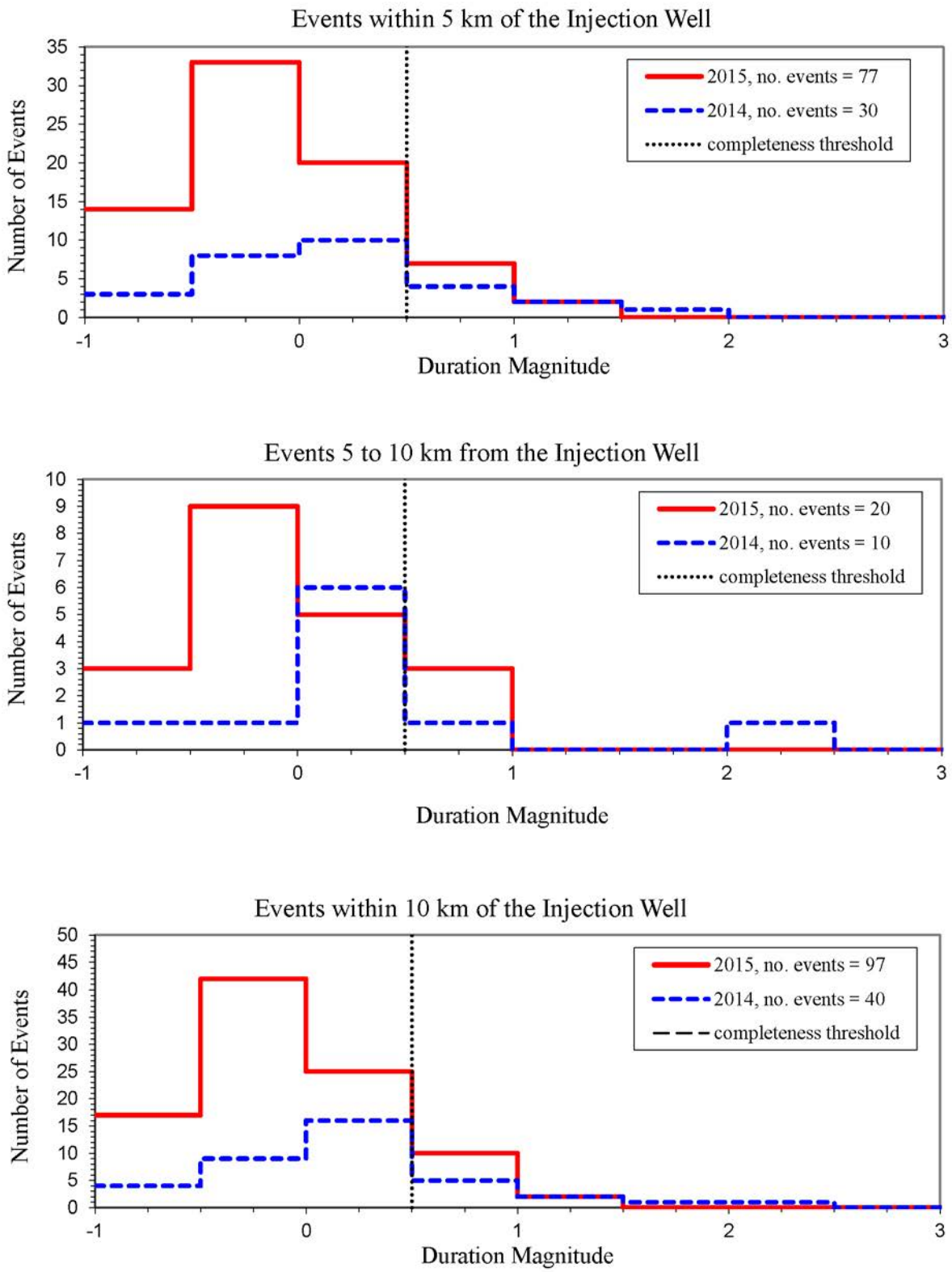

Figure 4-7: Magnitude histograms of events within 5 km of the injection well (top), at distances of 5 to 10 km from the well (middle), and in both regions (bottom) during 2015 (solid red lines) and 2014 (dashed blue lines).

4.3 Distant Earthquakes

During 2015, 35 likely-induced earthquakes were detected at distances greater than 10 km from the injection well. Most of these earthquakes occurred around the northern edge of Paradox Valley, a region where seismicity has been detected every year since 2000. Twenty-three events occurred in this northern-valley region in 2015, compared to only five events in 2014. However, the annual number of northern-valley events varies widely, ranging from 2 to 557 events per year since 2000. Hence, the increase from five events in 2014 to 23 events in 2015 is not unusual and is relatively minor compared to past swarms of northern-valley seismicity. The magnitudes of the 23 northern-valley earthquakes recorded during 2015 are comparable to the magnitudes of northern-valley events recorded in previous years. Magnitudes of the northern-valley earthquakes recorded from 2000 through 2014 range from M_D -0.8 to M_D 2.9, with all but one event having duration magnitude ≤ 2.3. Magnitudes of the earthquakes that occurred during 2015 range from M_D -0.9 to M_D 1.0. Twenty of the northern-valley earthquakes recorded in 2015 have estimated depths between 3.5 and 6.5 km (relative to the ground surface elevation at the injection wellhead). These values are comparable to estimated depths of previous northern-valley earthquakes having reasonably well-constrained hypocenters. The other three northern-valley earthquakes recorded during 2015 have larger depth estimates of between 8.4 and 8.7 km.

The 12 other distant earthquakes recorded during 2015 occurred in areas with little or no previous seismic activity. A cluster of nine earthquakes developed east of Paradox Valley, approximately 4 km east-northeast of seismic station PV12 (Figure 4-2). The first two events in this cluster occurred in August, 2015. Additional events were detected in October, November, and December. The magnitudes of these earthquakes range from M_D 0.0 to M_D 1.6, and their depths range from 5.2 km to 6.9 km. The remaining three distant events occurred on the southern edge of the valley; two of the events occurred 1 km southeast of seismic station PV02 and the third event occurred about 4.6 km northwest of PV02. The computed depths of these three events range from 4.7 to 5.6 km, and their magnitudes range from M_D 0.2 to M_D 1.4. Events were first detected in the vicinity of station PV02 in late 2014, at comparable depths. The lack of historical natural seismic activity in both of these regions and the relatively shallow depths of the events suggest that they are related to PVU fluid injection.

4.4 Historical Seismicity Trends

The rates and magnitudes of earthquakes that occurred during 2015 are compared to the historical seismicity trends in three plots described below. Only events with duration magnitude ≥ 0.5 (M 0.5+) are included in these plots, since the detection capability for earthquakes with magnitudes less than this threshold has varied considerably over the history of PVSN. First, the bubble plots in Figure 4-8 show the historical occurrence of shallow seismicity (< 10 km depth) as a function of date and earthquake magnitude during long-term injection at PVU (1996-2015). The area of each circle in these plots is scaled by the number of earthquakes in a given quarter-year and magnitude range. Individual bubble plots are included for earthquakes occurring within 5 km of the injection well, between 5 and 10 km from the well, and more than 10 km from the well. The downhole injection pressures, averaged over varying lengths of time, are included in Figure 4-8 for reference. In order to better observe the trends in recent years, similar plots that

only include data from 2008-2015 are presented in Figure 4-9. Lastly, we show the annual seismicity rates for 2008-2015, for the different distances from the well, in Figure 4-10.

These plots show that both the seismicity rate and maximum earthquake magnitude for the near-well area (within 5 km of the well) were relatively low in 2015. The maximum magnitude of events occurring within 5 km of the injection well was lower in 2015 (M_D 1.1) than in any previous calendar year since long-term PVU injection began in 1996 (Figure 4-8b). Annual near-well seismicity rates had been decreasing since 2009. In 2015, the near-well seismicity rate rebounded slightly but still remained low compared to historical trends (Figure 4-10a).

The seismicity rate and maximum earthquake magnitude observed at distances of 5 to 10 km from the injection well were also low during 2015 compared to previous years. Similar to the near-well region, the maximum magnitude of events occurring 5 to 10 km from the injection well was lower in 2015 (M_D 0.9) than in any previous calendar year since induced seismicity initiated at these distances in 1997 (Figure 4-8c). The annual rate of M 0.5+ earthquakes observed at distances of 5 to 10 km from the well during 2015 was also anomalously low, with only three such events being recorded. This rate is the same as that observed in 2014, but only 17% of the average annual rate observed from 2008 to 2013 (Figure 4-10b).

The annual rate of distant M 0.5+ events, those occurring more than 10 km from the injection well, has been increasing slightly for the past three years (Figure 4-10c). However, the rates still remain modest compared to historical trends. The maximum magnitude of the distant induced earthquakes in 2015 was M_D 1.6, which is comparable to maximum magnitudes in previous years.

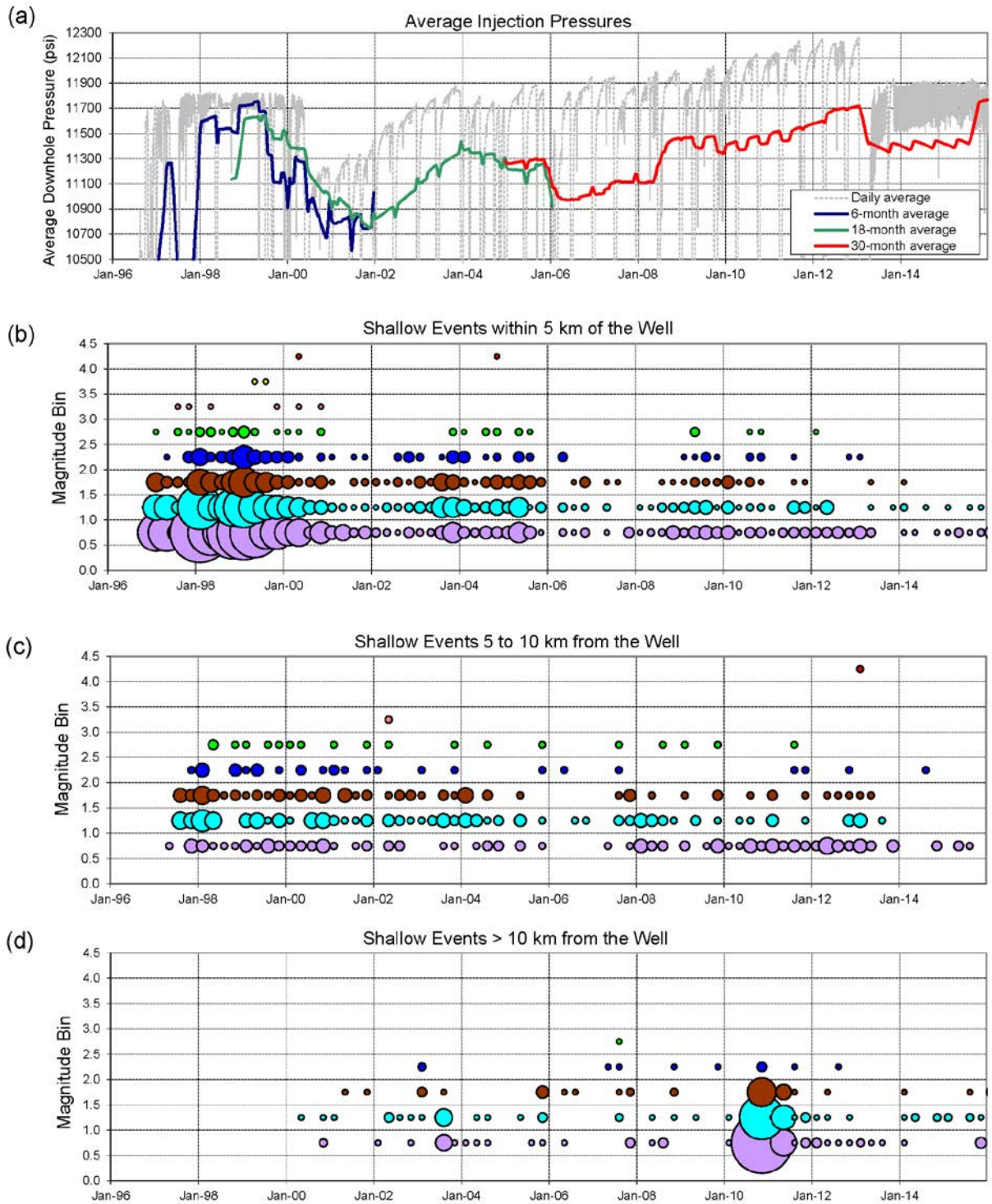

Figure 4-8: Injection well downhole pressure data averaged over daily, 6-month, 18-month, and 30-month time periods (a) and occurrence of shallow seismicity (depth < 10 km) as a function of date and magnitude within 5 km of the injection well (b), at distances of 5 to 10 km from the well (c), and more than 10 km from the well (d). In the seismicity plots, the area of each circle is scaled by the number of earthquakes in a given quarter-year and magnitude range; each plot is scaled separately.

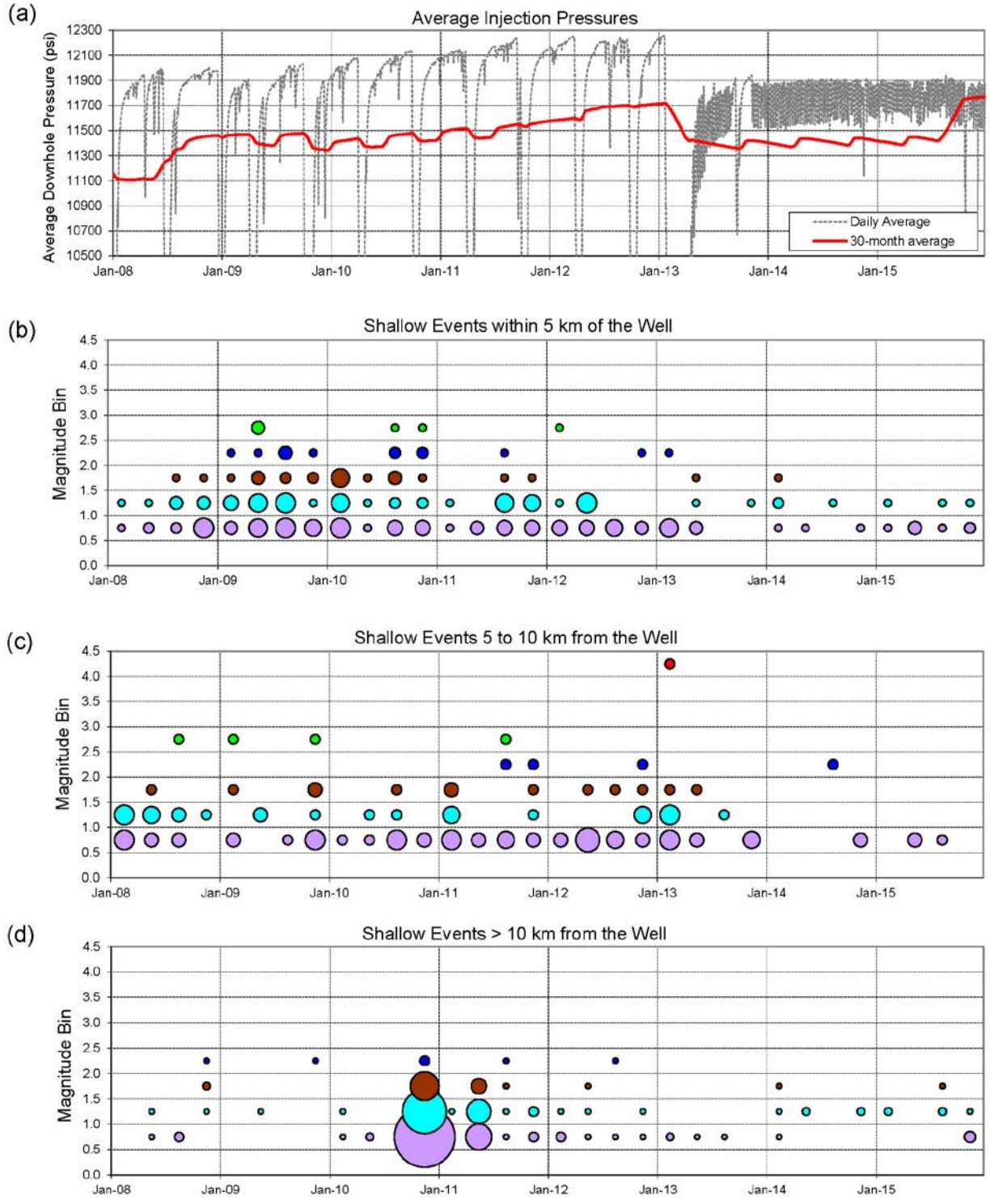

Figure 4-9: Same as Figure 4-8, but only showing data from 2008-2015.

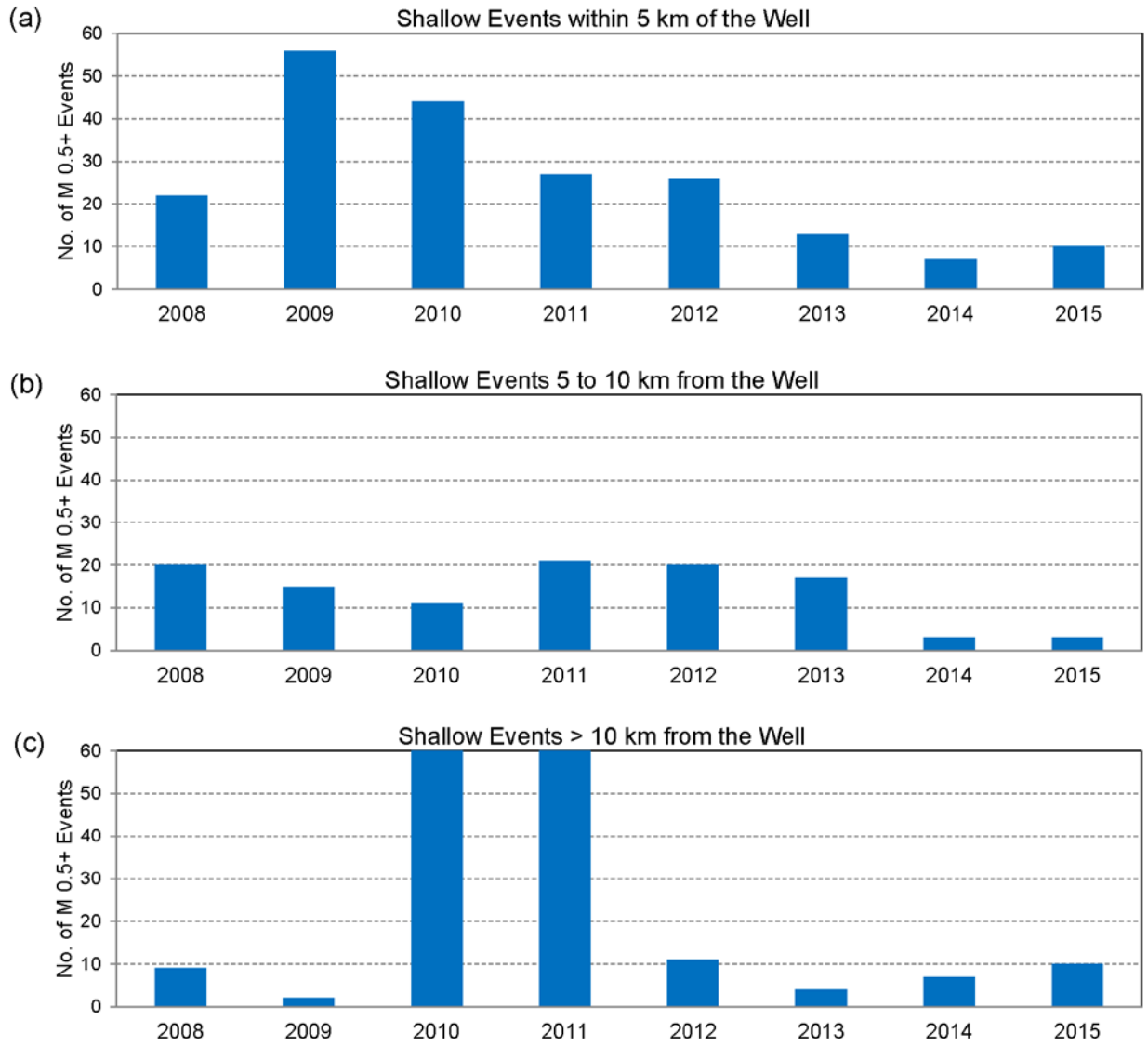

Figure 4-10: Annual number of shallow earthquakes (depth < 10 km) with $M_D \geq 0.5$ within 5 km of the injection well (a), 5 to 10 km from the well (b), and more than 10 km from the well (c). Data from 2008 to 2015 are shown. High counts in 2010 and 2011 for events more than 10 km from the well are clipped.

5 Conclusions

The rate of PVU-induced seismicity remained low in 2015 compared to historical trends. The number of M 0.5+ earthquakes observed within 10 km of the well during 2015 was 30% higher than the number observed in 2014, but still only 27% of the average annual rate observed during the preceding six years (2008 to 2013). The observed low seismicity rate within 10 km of the injection well is likely related to the three-month injection well shut-down in early 2013 and the subsequent changes in injection protocol (decreased flow rate and more frequent shut-in schedule). Stress re-distribution in the vicinity of the M 4.4 earthquake that occurred 8.2 km northwest of the injection well in January, 2013, could also be contributing to the current low seismicity rate in that region.

No induced earthquakes with magnitude ≥ 2.5 were recorded during 2015, and no events were reported as felt by the public. The largest earthquake induced in 2015 had a duration magnitude of 1.6 and occurred approximately 12 km northeast of the injection well, within a new cluster of induced seismicity that initiated in August, 2015.

6 References

Block, L., and C. Wood, 2009, *Overview of PVU-Induced Seismicity from 1996 to 2009 and Implications for Future Injection Operations,* Technical Memorandum No. 86-68330-2009-22, Bureau of Reclamation, Denver, Colorado, 16 pp.

Block, L.V., C. K. Wood, W. L. Yeck, and V. M. King, 2014, The 24 January 2013 M_L 4.4 earthquake near Paradox, Colorado and its relation to deep well injection, *Seismological Research Letters*, 85(3), 609-624.

Bremkamp, W., and C. L. Harr, 1988. *Area of Least Resistance to Fluid Movement and Pressure Rise, Paradox Valley Unit, Salt Brine Injection Project Bedrock, Colorado*, report to the Bureau of Reclamation, Denver, CO, 39 pp.

Earle, P.S., Bittenbinder, A., Bogaert, B., and Johnson, C.E., 2003, Turn to the worm: seismic network operation using the USGS Earthworm system: ORFEUS Newsletter, v. 5, no. 1.

Fenneman, N. M., and D. W. Johnson, 1946, Physiographic divisions of the conterminous U. S., USGS, Washington D.C., 1:7,000,000-scale Map, USGS Digital Version, 2002

Friberg, P., Lisowski, S., Dricker, I., and Hellman, S., 2010, Earthworm in the 21st century, in EGU General Assembly 2010, Vienna, Austria, p. 12654.

Gibbs, J.F., Healy, J.H., Raleigh, C.B., and Coakley, J., 1973, Seismicity in the Rangely, Colorado, Area: 1962-1970: Bulletin of the Seismological Society of America, v. 63, no. 5, 1557-1570.

Hsieh, P.A., and Bredehoeft, J.D., 1981, A reservoir analysis of the Denver earthquakes; a case of induced seismicity: JGR. Journal of Geophysical Research. B, v. 86, no. 2, p. 903-920.

Johnson, C.E., Bittenbinder, A., Bogaert, B., Dietz, L., and Kohler, W., 1995, Earthworm: A Flexible Approach to Seismic Network Processing: IRIS Newsletter, v. XIV, no. 2, 1-4.

Kharaka, Y. K., G. Ambats, J. J. Thordsen, and R. A. Davis, 1997, Deep well injection of brine from Paradox Valley, Colorado: Potential major precipitation problems remediated by nanofiltrations, *Water Resour. Res*., 33(5), 1013-1020.

Nicholson, C., and Wesson, R.L., 1990, Earthquake Hazard Associated With Deep Well Injection - A Report to the U.S. Environmental Protection Agency: U.S. Geological Survey Bulletin 1951, 86 pp.

O'Connell, D.R.H, 2008, Probabilistic Seismic Hazard Analysis, Hungry Horse Dam, Hungry Horse Project, Montana, Technical Memorandum No. 86-68321-2008-12, Bureau of Reclamation, Technical Service Center, 89 pp.

Raleigh, C.B., Healy, J.H., and Bredehoeft, J.D., 1976, An Experiment in Earthquake Control at Rangely, Colorado: Science, v. 191, no. 4233, 1230-1237.

Wood, C., V. King, L. Block, and W. Yeck, 2015, The M_L 4.4 Earthquake of January 24, 2013, Near Paradox, Colorado, and Implications for Near-term Injection Operations, Draft Technical Memorandum No. 86-68330-2013-12, Bureau of Reclamation, Denver, Colorado, 151 pp.

Appendix A

2015 Site Visit Report

Paradox Valley Seismograph Network

Site Visit Summary

Site Visit No: PVSN-2015-1 Departure Date: 07/27/2015 Return Date: 08/06/2015

PURPOSE:

Several activities were undertaken during this maintenance trip including station removals, battery replacements, GPS repairs, grounding system upgrades, review of radio configurations for stations with weak wireless communication links, and replacement of failed battery backup system at the communication hub at Hopkins Field.

WORK SUMMARY:

All vestiges of analog seismograph stations PV08 and PV09 were removed. PV08 was removed at the request of the National Forest Service to accommodate interests of the Ute Tribes where the location may be a part of a vision quest circle. Two stations, PV21 and PV23, were down for several months. These stations were successfully repaired and brought back online. Batteries more than 5 years old were replaced at several sites. Three stations, PV22, PV07, and PV12, had problematic GPS timing systems which were resolved by a power cycle of GPS break-out-box (BoB) at two sites and replacement of the GPS BoB at one site. Grounding systems were upgraded at several stations with the most important upgrade occurring at the PV12 repeater station. Radio communication (comm) links were reviewed at three stations: PV21, PV05, and PV20. We were successful in improving the comm links at stations PV21 and PV05 but the PV20 comm link is still problematic. At the communication hub, we upgraded the private network switch, initially configured *Earthworm* on the *Windows* system to prepare it for the transition from the Linux SUSE system to the *Windows* 2008 server system. At that point only one server will be operating, managed under the BOR domain.

PERSONNEL:

Glenda Besana-Ostman, Mike Gilliam, Justin Schwarzer, and Mark Meremonte

ACTIVITIES BY SITE:

<u>Comm Hub</u>

- Replaced failed APC-1500 with new APC-1500.
- Grounded cable bridge. This completes all the grounding required by Motorola for the comm hub and tower.
- Installed *Earthworm* on the *Windows* 2008 Server computer. It will be tested before finalizing the *Earthworm* move from the old Penquin server. Once testing is complete and successful, then *Earthworm* and *Scream* will be running on single computer system, facilitating management.
- Removed old *Windows* 2003 server.
- Replaced Linksys SD-205 switch on the private network with ADAM-6520 industrial switch.
- The T1 dedicated phone line from Hopkins Field to Denver was down for almost two days due to a lightning strike near Hopkins Field. The T1 lines to the Federal Aviation Administration (FAA), the airport terminal, and the sheriff's office were also down. The Nucla Naturita Telephone Company (NNTC) indicated that the lightning struck the tower at the airport, but there were no signs of damage to the PVSN Comm Hub facility or to FAA's facility. NNTC indicates that it will replace hard-wire with fiber-optic in the near future.

- Down time span: 08/02 17:08:13 to 08/04 14:49:32 MDT or about 1 day, 21 hours, 41 minutes

<u>PV08 and PV09 analog stations</u>

- Both stations have been dismantled with total removal of concrete bases
  - Reclamation has a state lease at PV09 which can be cancelled now; Andy Nicholas is looking into the lease to verify this.
  - Linda Bledsoe of the U.S. Forest Service has been informed of PV08's removal. She thanks us much for its removal but also informs us that stations PV08 and PV15 were authorized under one permit. We are looking into the possibility of closing this permit and reissuing a new permit for PV15 on Pinto Mesa.

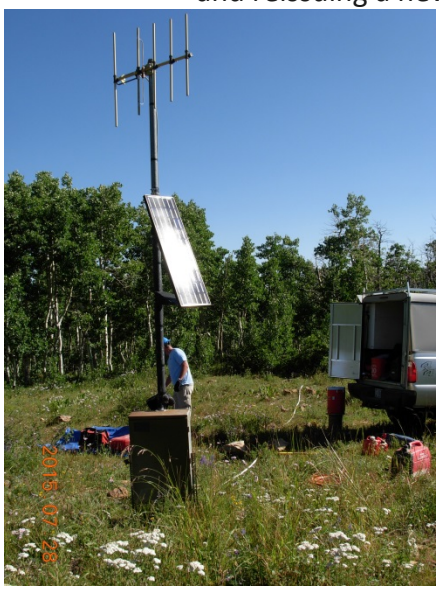

a) Shelter before removal

b) Shelter location after removal

c) Vaults before removal

d) Vault location after removal

- Four S13 seismometers were removed in total.

PV21

- The DM24 BoB with upgraded fuses failed, causing no communication to the datalogger; it was replaced with another DM24-BoB with upgraded fuses;
    - The station was brought back online after being down since mid-December, 2014.
- A spline ball was installed.
    - The grounding system is complete at this site.
- Vegetation mitigation was performed to facilitate line-of-site communication. As a result, communication dropouts have been reduced.

PV23

- The DM24-BoB with upgraded fuses failed, causing no communication to the datalogger; it was replaced with another DM24-BoB with upgraded fuses
    - The station was brought back online after being down since March, 2015.
- The COAX cable was replaced with steel conduit protection to prevent future bear damage.

Comment: The grounding system is complete at this site.

PV12

- GPS timing failed on August 1; a power cycle on August 3 restored GPS timing.
- Six batteries were replaced.
- Two spline balls and a star array grounding system were installed.
    - The grounding system is complete at this site.
- The omni antenna was raised 1.5 feet and re-oriented on the tower to facilitate line-of-site communication to station PV20.
- Vegetation mitigation was performed to improve line-of-site communication to station PV20.
- The DM24-BoB without upgraded fuses was replaced with a DM24-BoB with upgraded fuses.
    - However, the new BoB induced high frequency noise onto the seismic signal. Therefore, the old BoB was re-installed for now.

PV02

- Six batteries were replaced.
- The omni antenna was raised 1.5' and re-oriented on the tower to facilitate line-of-site communication to station PV05. Currently, communication dropouts from PV05 have been reduced.
- Vegetation mitigation was performed to improve line-of-site communication to station PV05.
- Five gallons of water were added to the chem-rod grounding system.

Comment: The grounding system is complete at this site.

- The old S13 seismometer and electronics were removed from both the station and repeater shelters; the vault, shelters, and masts still remain.

PV04

- Six batteries were replaced.
- An additional ground rod was installed to configure a star grounding array.
    - Two spline balls and copper (Cu) and aluminum (Al) cables still need to be installed.

PV10, PV11, PV14, PV17

- Three batteries were replaced at each site.

Comments: Station PV11 needs a DM24-Bob upgrade.
The grounding systems still need to be completed at these sites.

PV07

- The GPS-Bob was power cycled to re-establish GPS timing.
- The DM24-BoB was old style and was replaced with a DM24-BoB with upgraded fuses.
- The S13 seismometer and electronics were removed; the vault, shelter, and mast still remain.

Comments: The solar system is still charging batteries here for now.
The grounding system still needs to be completed.

PV15

- Installed grounding star array with Cu braid cable (no spline ball here).
    - The grounding system is complete at this site.
- The S13 seismometer and electronics were removed; the vault, shelter, and mast still remain.

PV22

- The GPS-Bob failed due to a broken power wire inside the box. The GPS-Bob was replaced, taking care to remove and reattach the wire connections.

Comment: The grounding system here still needs to be completed with a spline ball and Cu plates.

PV20

- A 6-element antenna was replaced with a 7-element antenna to provide more gain with comparative radiation. The antenna was slightly angled up to point directly at PV12's location on the mesa and over shoot the intervening tall ridge between stations PV20 and PV12.
    - Results were mixed with no significant change of the RSSI (-84 to -87 dBm) or signal-to-noise ratio (S/N) (23 to 24 dB).
- A 12-element antenna was also tested. This antenna has higher gain and a tighter radiation pattern oriented horizontally about 6 degrees to North away from the obstructing ridge between PV20 and PV12.
    - Initially the results were better, with a RSSI of -81 to -85 dBm and the S/N still low at 23 dB, but this degraded over time.
    - Possibly this angle may have caused the radio to sometimes attempt to associate with station PV04.
    - We finally switched this antenna out for the 7-element antenna discussed above.
- We also tested a different polyphaser in case it was blown or degraded but no effect was observed.

Comment: The grounding system still needs to be completed at this site.

Strong Motion Stations

PVEF

- The K2 datalogger and sensor were pulled.
    - This equipment was tested in the lab to verify the erratic behavior and identify the components responsible.

- The K2 was sent in for repair.

PVPP

- This station was inspected.
  - The phone cable is installed above ground.
  - Several splices are visible, presumably related to animal damage.
  - The phone box is a mess of unruly wiring and unused/disconnected wires.

Comments: If we keep this phone line, it needs to be installed better. There may be an underground cable that could be utilized; this needs to be verified.

Appendix B

Evaluation of PVSN Event Detection

Summary

PVSN's event detection capabilities vary over time. The magnitude completeness threshold, the minimum earthquake magnitude for which all events are reliably detected and recorded, is an important parameter used to quantify a seismic network's event detection capabilities. The magnitude completeness threshold at any given time depends on many factors, including the number of seismic stations operating, background seismic noise levels, the robustness of real-time data transmission, and several parameters set within the data acquisition software that continuously monitors the waveform data streams in real time.

In early 2015, during testing for a software upgrade (described in section 3.3), we became aware that PVSN's event detection was degraded and that its magnitude completeness threshold may have changed. After thorough analysis of log files generated by the data acquisition software, we determined that the change in event detection was related to physical changes in the seismic network. In addition, we identified a parameter in the data acquisition software that could be adjusted to compensate for these physical changes. This adjustment was implemented on May 1, 2015, and PVSN's event detection capabilities were improved.

To evaluate how significantly PVSN's event detection capabilities had been affected, we subsequently retrieved and re-processed continuous PVSN waveform data for a period of approximately 5.5 months. We specifically wanted to determine whether the magnitude completeness threshold previously used in multi-year analyses of PVSN seismic data (M_D 0.5) had been compromised. Results of these analyses demonstrate that induced earthquakes with magnitude $\geq M_D$ 0.5 had been detected reliably even during the period of degraded event detection, and hence the magnitude completeness threshold used for long-term seismic data analyses was not compromised. In contrast, detection of events with magnitude $< M_D$ 0.5 had been substantially degraded for at least nine months and possibly for a few years.

PVSN Event Detection Analyses

PVSN automatic event detection is performed within the data acquisition software *Earthworm*, a widely used open-source seismic data acquisition software package (Johnson and others, 1995; Earle and others, 2003; Friberg and others, 2010). Automatic event detection is performed in two steps (Johnson, 1979): (1) triggering of individual seismic stations based on changes in the short-term to long-term average signal levels, and (2) detection of a seismic event based on a given number of triggered stations within a specified time window. Step 2 is performed for multiple station subnets, which typically are groups of adjacent seismic stations. Subnets are created to increase triggering sensitivity in geographic areas of greatest interest, such as near the injection well. Triggered seismic events can include naturally-occurring or induced earthquakes within or near the perimeter of the network (local earthquakes), earthquakes occurring 30 km or more outside the perimeter of PVSN in Colorado and Utah (regional earthquakes), earthquakes with M > ~5 occurring at great distances (teleseismic earthquakes), blasts from mining or construction activities, and noise triggers generated by non-earthquake sources (e.g., vehicles, sonic booms, wind, thunder, or electrical noise). Recording of the first category, local earthquakes, is the primary purpose of the Paradox Valley Seismic Network. Once a seismic event has been detected and recorded, subsequent post-processing of the detected seismic event is required to identify the type of the event, and for local earthquakes, to perform detailed interactive analyses.

In early 2015, while trying to resolve differences in event triggers from two different versions of *Earthworm* in preparation for a software upgrade (section 3.3), we discovered that the event detection was not consistently being performed correctly by either version. Review of the log files created by the *Earthworm* modules that perform the station and subnet triggering indicated that, while the station triggering was being done identically by the two versions of *Earthworm,* the subnet triggering was often not being done correctly by either version. After detailed analyses of the log files, we determined that *Earthworm* was sometimes performing the subnet triggering before the data from all of the seismic stations had a chance to arrive at the *Earthworm* computer. Unfortunately, *Earthworm* does not have the ability to go back in time to re-evaluate the subnet triggering if data packets from a particular seismic station arrive too late.

Since Earthworm only performs the event detection process once for a given data time window, the software accommodates possible delays in seismic data transmission by providing a parameter, called *latency*, that specifies a time delay before executing the subnet triggering algorithm. In addition, a second parameter, *TimetoLive,* is provided to account for the propagation time of seismic waves across the stations in a seismic network; this parameter essentially lengthens the effective time window for event detection. Prior to 2015, the *latency* parameter had been set to 1 second and the *TimetoLive* parameter had been set to 10 seconds for the PVSN analog stations and 15 seconds for the PVSN digital stations. The small *latency* value was adequate when PVSN consisted primarily of analog seismic stations because all data streams were digitized and time-stamped simultaneously at the communication hub at Hopkins Field in Nucla, Colorado, just prior to being sent to *Earthworm* for analysis. Hence, there was a negligible time delay between the data time stamp and the time that *Earthworm* did the subnet processing time for a data packet. When individual stations were converted to digital, the data packets were time-stamped by the GPS clock at each station, and then sent asynchronously by radio to Hopkins Field. Hence, the delay between when the data streams were time-stamped and when they were processed by *Earthworm* increased, and the amount of the increase depended on several factors such as radio interference, data compression, and communications network load. In July, 2014, two things occurred that may have caused these delays to have a greater impact on event detection. First, all of the remaining analog stations, which had been providing some data for event detection, were taken offline. Hence, PVSN's event detection became entirely dependent on the delayed digital station data packets. At the same time, the radio antennas receiving the data at the Nucla hub were moved to a new tower. For several seismic stations, radio data transmission was less robust on the new tower than on the old tower, which resulted in increased data packet delays because more of the data had to be retransmitted.

In order to determine an appropriate value for the *latency* parameter, as well as to evaluate how the station radio transmission time delays had varied over time and therefore indirectly infer how PVSN's event detection may have qualitatively varied over time, we developed a code for automatically scanning the *Earthworm* log files and computing the daily average lag time for each station. This station lag time is defined as the time difference between the time stamp of a data packet (the GPS time stamp which occurs at the seismic station) and the computer system time when the data are received by *Earthworm*.

The daily average lag times for the 20 digital PVSN seismic stations from mid-2013 through 2015 are shown in Figure B-1 to Figure B-4 . Average lag times vary substantially from day to day, as demonstrated by the dashed gray curves in Figure B-1 to Figure B-4. In order to better observe the longer-term variations in station lag times, centered 9-day running average curves were computed; these are the solid red curves in Figure B-1 to Figure B-4. Lag times vary substantially among the 20 digital PVSN seismic stations. The stations with the most robust radio telemetry (e.g., PV04, PV07, PV15,

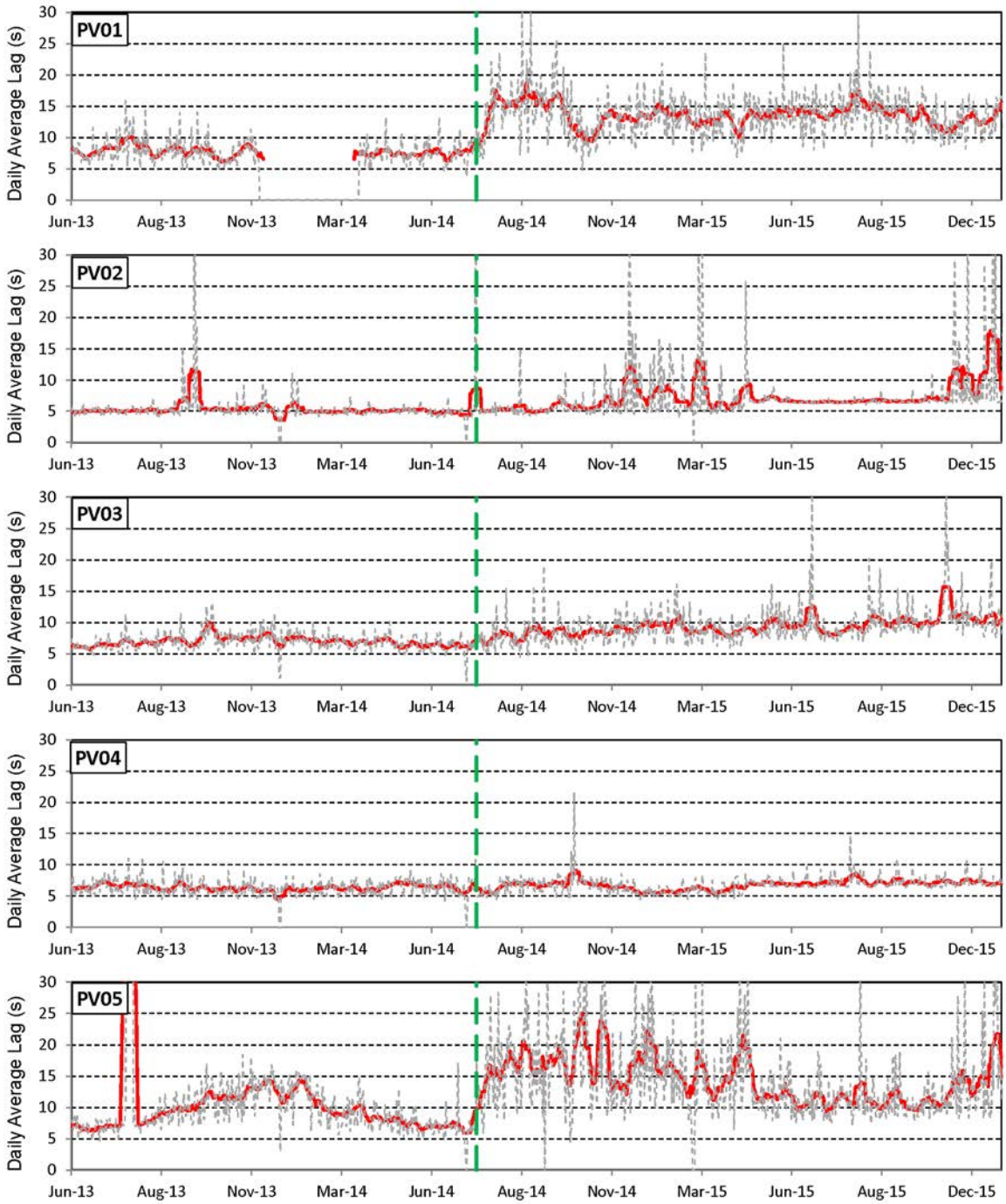

Figure B-1: Daily average lag times of digital stations PV01, PV02, PV03, PV04, and PV05. The dashed gray curves are the daily average lag times; the solid red curves are centered 9-day running averages of the dashed curves. The vertical dashed green lines indicate the time when the radio antennas were moved to a new tower at the communication hub.

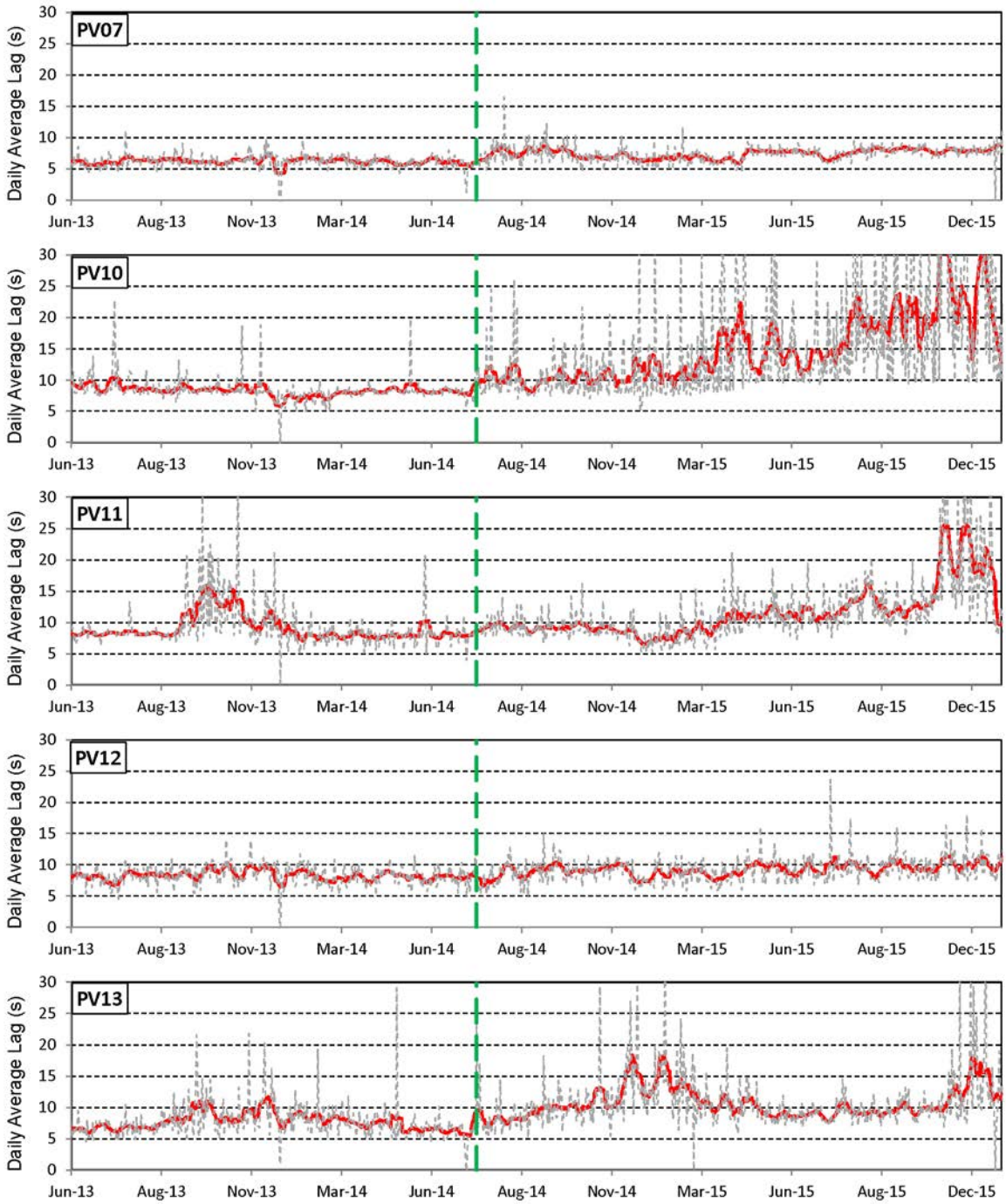

Figure B-2: Daily average lag times of digital stations PV07, PV10, PV11, PV12, and PV13. The dashed gray curves are the daily average lag times; the solid red curves are centered 9-day running averages of the dashed curves. The vertical dashed green lines indicate the time when the radio antennas were moved to a new tower at the communication hub.

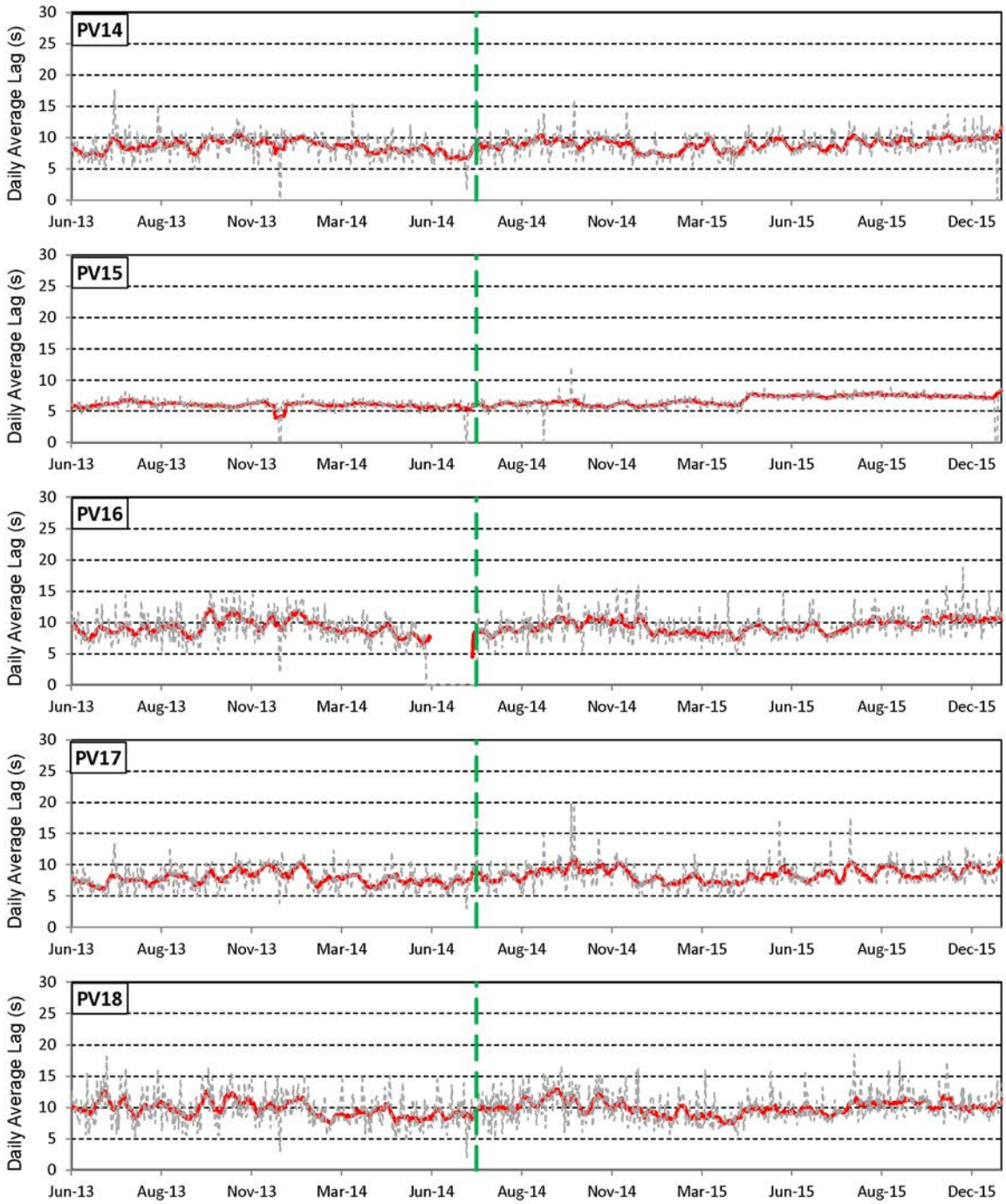

Figure B-3: Daily average lag times of digital stations PV14, PV15, PV16, PV17, and PV18. The dashed gray curves are the daily average lag times; the solid red curves are centered 9-day running averages of the dashed curves. The vertical dashed green lines indicate the time when the radio antennas were moved to a new tower at the communication hub.

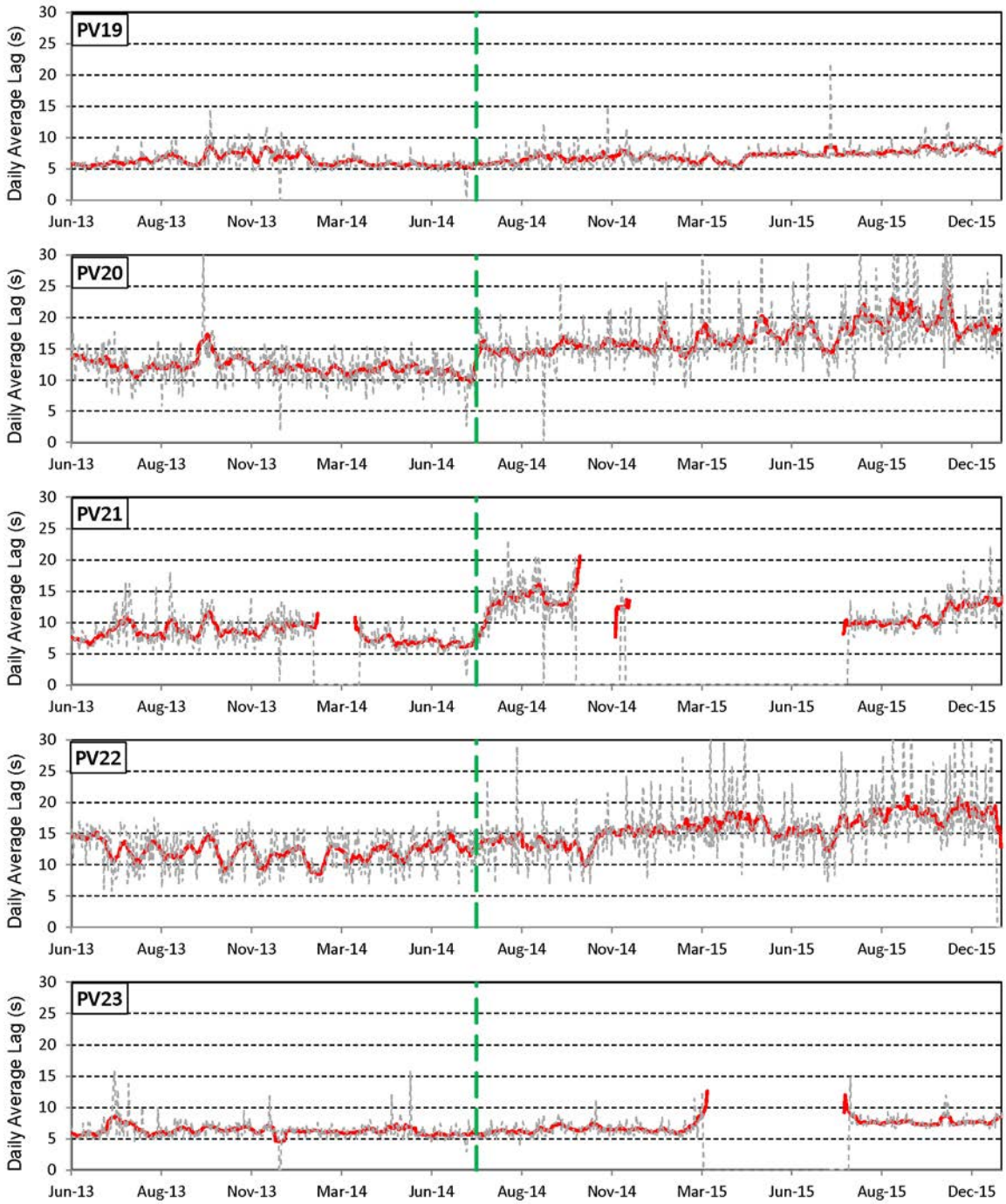

Figure B-4: Daily average lag times of digital stations PV19, PV20, PV21, PV22, and PV23. The dashed gray curves are the daily average lag times; the solid red curves are centered 9-day running averages of the dashed curves. The vertical dashed green lines indicate the time when the radio antennas were moved to a new tower at the communication hub.

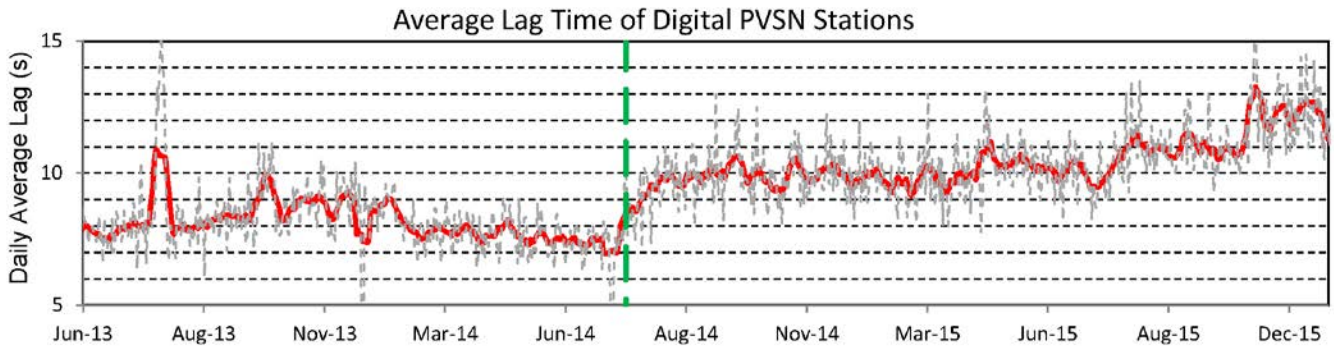

Figure B-5: Daily average PVSN digital network lag time. This network curve was computed from averaging the individual station lag times shown in Figure B-1 to Figure B-4 and does not include the near-zero lag times of the analog stations that were online until mid-July, 2014. The dashed gray curve is the daily average lag time; the solid red curve is a centered 9-day running average of the dashed curve. The vertical dashed green line indicates the time when the radio antennas were moved to a new tower at the communication hub.

PV19, and PV23) have lag times generally less than 8 seconds. The stations with less robust radio telemetry (e.g., PV01, PV05, PV10, PV13, PV20, PV21, and PV22) have lag times up to about 18-20 seconds. Several of these stations also show a substantial increase in lag time after July, 2014, when the radio antennas were moved to the new tower at the communication hub. The daily average network lag time, computed by averaging the individual lag curves for the digital stations, increased from ~8 seconds to ~10 seconds at this time (Figure B-5). This network average curves does not include the near-zero lag times of the analog stations which were online prior July, 2014. If the lag times from the analog stations were included, the average network lag time prior to July, 2014 would be about 6 seconds.

Based on the station lag data discussed above, the *latency* parameter in Earthworm was increased to 30 seconds beginning on May 1, 2015. Analyses of *Earthworm*-generated log files recorded after this date indicate that the subnet triggering was subsequently working correctly, and triggers from both *Earthworm* versions were consistent.

To evaluate how much the degraded event detection capabilities affected the detection of local induced earthquakes of interest, we re-processed continuous PVSN waveform data recorded during the 5.5-month period immediately prior to the adjustment in the *latency* parameter (mid-November, 2014 to the end of April, 2015). Data from this time window were analyzed because these data were readily available and because it was thought that analysis of data from this time period would give the "worst case scenario". That is, based on the lag time patterns shown in Figure B-1 to Figure B-5, event detection for earlier time periods should have been as good as or better than that during the time period examined. Waveform data files from 11/11/2014 to 4/30/2015 were re-processed using the *tankplayer* module within *Earthworm.* (Data files for the days of 12/11/2014-12/14/2014 and 1/2/2015 produced errors and therefore could not be re-processed.) The *tankplayer* feature allows previously-recorded continuous waveform data to be fed into *Earthworm* and processed in the same manner as it is when the data are recorded in real time. When performing the *tankplayer* analysis, we used the same event detection algorithms and parameters as before, except that any negative effects of late-arriving data were eliminated. Hence, this processing produced the triggered event files that would have been obtained with an infinite *latency* parameter. In this way, we were able to recover all seismic events that were originally missed for this time period.

Manual review and processing of the seismic events produced by the *tankplayer* analysis was performed, and the local earthquakes retrieved were then compared to the events in the original local earthquake catalog for the same days. Twenty-four local earthquakes were originally recorded for this time period, ranging in duration magnitude from M_D -0.6 to M_D 1.1. During the *tankplayer* analysis, all of the original 24 earthquakes were detected, along with 16 new likely-induced earthquakes. The new earthquakes range in magnitude from M_D -1.2 to M_D 0.2. The origin times, magnitudes, and locations of these new events are listed in Table B-1. A histogram comparing the number of local earthquakes by magnitude for the final catalog compared to the originally recorded events is shown in Figure B-6. The greatest increase in number of detected earthquakes in the final catalog is for events with magnitudes less than M_D 0.0, and there is no change for events with $M_D \geq 0.5$. The histogram in Figure B-7 shows the percent of the events in the final catalog that were originally missed because of the degraded event detection. Zero percent of events with $M_D \geq 0.5$ were missed; 31% of events with $M_D \geq 0.0$ and < 0.5 were missed; 62% of events with $M_D \geq -0.5$ and < 0.0 were missed; and 67% of events with $M_D \geq -1.0$ and < -0.5 were missed.

Table B-1: New events detected by the *tankplayer* analysis.

Date	Time[1]	Latitude, deg. N	Longitude, deg. W	Elevation[2] (km)	Depth[3] (km)	Magnitude[4]
11/14/14	9:55:31	38.2832	-108.9051	-2.0	3.5	0.1
11/26/14	0:05:34	38.2707	-109.0528	-0.5	2.0	-0.7
11/26/14	0:05:45	38.2733	-109.0522	-0.7	2.2	-1.2
12/16/14	15:41:43	38.2864	-108.9134	-1.2	2.8	-0.2
12/21/14	9:05:12	38.3215	-108.9862	-2.3	3.8	0.1
12/23/14	19:54:17	38.2825	-108.9160	-1.2	2.8	-0.7
1/20/15	14:17:08	38.3056	-108.8965	-2.7	4.3	-0.1
2/13/15	13:59:50	38.2772	-108.8273	-2.4	4.0	-0.1
2/13/15	15:15:56	38.2772	-108.8268	-2.5	4.0	0.0
2/16/15	10:37:59	38.3392	-108.8615	-5.2	6.7	-0.5
3/5/15	9:00:20	38.2696	-108.8665	-1.2	2.7	0.0
3/11/15	14:09:41	38.4175	-108.9255	-2.3	3.8	0.2
4/1/15	4:05:49	38.2755	-108.8990	0.3	1.2	-0.1
4/9/15	3:41:11	38.2772	-108.9260	-0.7	2.2	-0.4
4/16/15	5:35:46	38.2727	-108.8595	-2.1	3.6	-0.5
4/23/15	0:44:12	38.3325	-108.8615	-4.6	6.2	-0.3

[1] Time listed is Coordinated Universal Time, UTC (Mountain Standard Time = UTC – 7 hours; Mountain Daylight Savings Time = UTC – 6 hours)
[2] Elevation is given with respect to mean sea level.
[3] Depth is referenced to the surveyed elevation of the injection wellhead, 1.524 km.
[4] Magnitudes listed are duration magnitudes

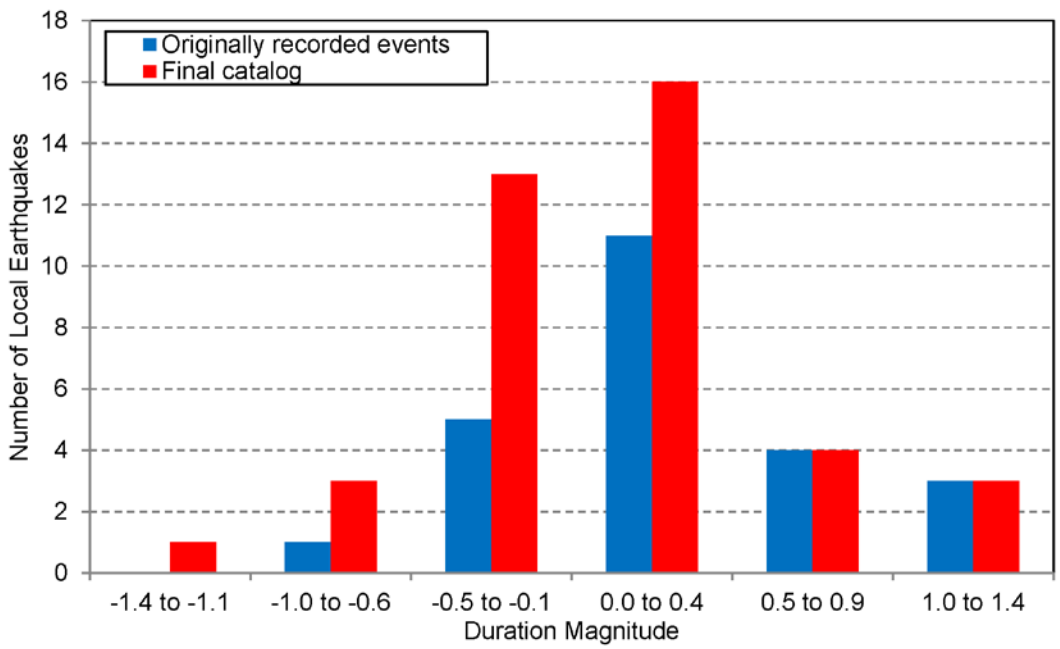

Figure B-6: Number of local earthquakes originally recorded (blue bars) and number of local earthquakes in the final catalog (red bars) by magnitude, for the time period of 11/11/2014 to 4/30/2015. All of the events that were originally missed have magnitudes less than M_D 0.5.

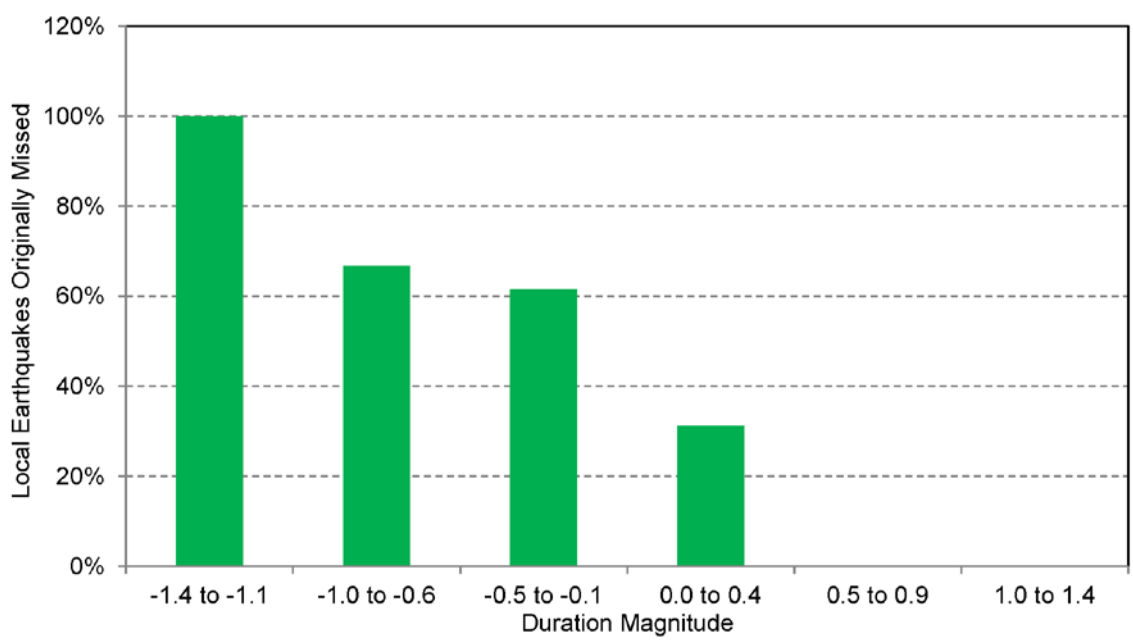

Figure B-7: Percent of local earthquakes from 11/11/2014 to 4/30/2015 that were originally undetected due to degraded event detection.

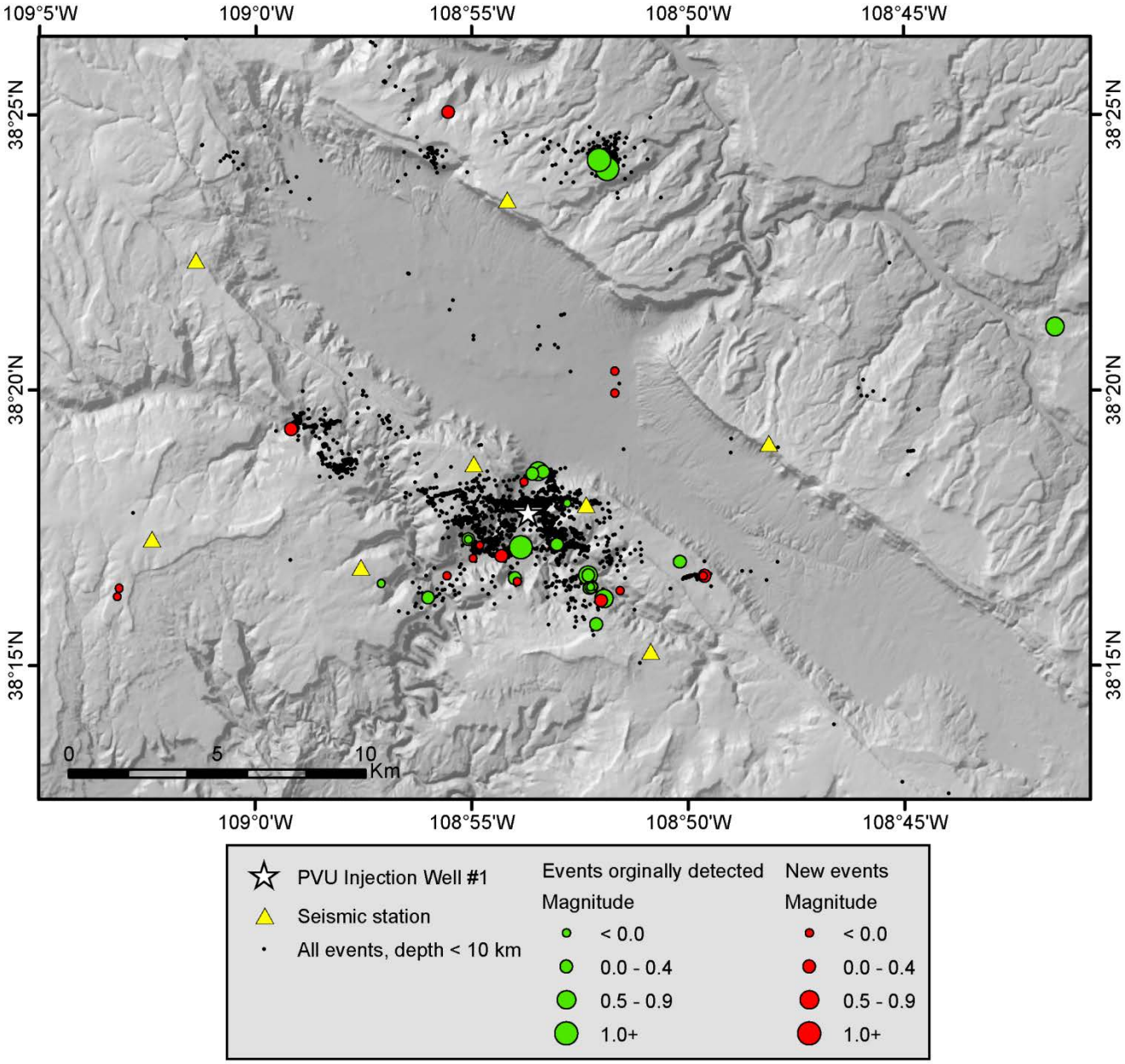

Figure B-8. Location of the local earthquakes originally recorded and the new events detected during the time period of the *tankplayer* analysis.

The locations of the new events recovered from the *tankplayer* analysis, along with the locations of the 24 events originally detected for the same time period, are shown in Figure B-8. The historical induced earthquakes are included in Figure B-8 for reference. Hypocenter depths of the new events range from 1.6 to 7.0 km, consistent with depths of other induced events. New events were detected in nearly all areas of previous induced seismicity, including the near-well area, the NW and SE clusters, the northern valley area, and central Paradox Valley. In addition, two events were detected about 12.5 west of the injection well, near seismic station PV10 (Figure B-8). No previous shallow events (depth < 10 km) had been detected in this area. The depths of these two events, which occurred on November 26, 2014, are 2.0 and 2.2 km (Table B-1), and these events are considered to be likely induced by PVU injection.

In addition to the 16 new events described above, two previously undetected M_D 1.1 earthquakes outside the bounds of PVSN were also recovered by the *tankplayer* analysis, at distances of 44 km and 63 km from PVU Injection Well #1. These earthquakes have estimated depths of 17.7 km and 22.5 km, respectively. Their depths and locations indicate that these events are probably natural, not induced. Detection thresholds for events outside the bounds of PVSN are higher than for events inside the network, as they generally need to trigger at least four seismic stations, and the closest four seismic stations may be tens of kilometers away. For these events, the closest four stations were at distances of 26 to 41 km for the first event and 45 to 59 km for the second event. Thus, the failure of the network to trigger on these events should not be taken as an indication that the network would not have triggered on induced events of similar magnitudes.

The results presented above indicate that the magnitude completeness threshold previously used for multi-year analyses of PVU induced seismicity data, M_D 0.5, was not compromised by the degraded PVSN event detection capabilities in 2014-15. Although we have not re-processed continuous waveform data recorded prior to mid-November, 2014, we can infer that the PVSN event detection capabilities prior to November, 2014 were similar to or better than that for the time period evaluated (November, 2014 – April, 2015), based on the station and network lag time trends discussed earlier (Figure B-1 to Figure B-4). Detection of events with magnitude < M_D 0.5 was substantially degraded for a period of at least nine months (mid-July, 2014 – April, 2015), and possibly for a few years.

References

Earle, P.S., Bittenbinder, A., Bogaert, B., and Johnson, C.E., 2003, Turn to the worm: seismic network operation using the USGS Earthworm system: ORFEUS Newsletter, v. 5, no. 1.

Friberg, P., Lisowski, S., Dricker, I., and Hellman, S., 2010, Earthworm in the 21st century, in EGU General Assembly 2010, Vienna, Austria, p. 12654.

Johnson, C.E., 1979, I. CEDAR -- an approach to the computer automation of short-period local seismic networks: Pasadena, CA, California Institute of Technology, Ph.D.

Johnson, C.E., Bittenbinder, A., Bogaert, B., Dietz, L., and Kohler, W., 1995, Earthworm: A Flexible Approach to Seismic Network Processing: IRIS Newsletter, v. XIV, no. 2, p. 1-4.

Appendix C

PVSN 2015 Local Earthquake Catalog

Table C-1: Local earthquakes recorded by PVSN during 2015

Date	Time[1]	Latitude (deg.)	Longitude (deg.)	Elevation[2] (km)	Depth[3] (km)	M[4]	Distance from Injection Well (km)	Old Location Category[5]
1/6/15	23:14:05	38.2813	-108.8365	-3.1	4.6	0.3	5.4	SE cluster
1/9/15	3:19:27	38.3525	-108.6917	-8.8	10.3	0.9	18.8	other
1/13/15	10:38:24	38.2883	-108.9178	-1.1	2.7	-0.4	2.2	near-well
1/13/15	15:50:24	38.2882	-108.9177	-1.1	2.7	0.0	2.2	near-well
1/20/15	14:17:08	38.3056	-108.8965	-2.7	4.3	-0.1	1.0	near-well
1/21/15	13:51:08	38.2773	-108.8717	-0.9	2.5	0.9	3.0	near-well
1/21/15	15:56:54	38.4005	-108.8643	-3.5	5.0	1.0	11.8	N. valley
1/22/15	1:46:49	38.2773	-108.8716	-0.9	2.5	0.0	3.0	near-well
1/22/15	3:37:50	38.2740	-108.8698	-1.7	3.2	-0.4	3.3	near-well
2/4/15	0:03:32	38.4030	-108.8676	-3.6	5.1	1.0	12.1	N. valley
2/5/15	0:40:08	38.3081	-108.8931	-2.7	4.2	0.2	1.3	near-well
2/13/15	13:59:50	38.2772	-108.8273	-2.4	4.0	-0.1	6.3	SE cluster
2/13/15	15:15:56	38.2772	-108.8268	-2.5	4.0	0.0	6.3	SE cluster
2/16/15	10:37:59	38.3392	-108.8615	-5.2	6.7	-0.5	5.6	central valley
2/27/15	23:12:04	38.2858	-108.8975	-2.0	3.6	1.1	1.2	near-well
3/5/15	9:00:20	38.2696	-108.8665	-1.2	2.7	0.0	3.9	near-well
3/11/15	14:09:41	38.4175	-108.9255	-2.3	3.8	0.2	13.7	N. valley
4/1/15	4:05:49	38.2755	-108.8990	0.3	1.2	-0.1	2.4	near-well
4/4/15	19:56:59	38.2736	-108.8712	-1.0	2.6	0.2	3.3	near-well
4/4/15	22:17:58	38.2740	-108.8707	-1.1	2.7	-0.2	3.3	near-well
4/4/15	22:19:11	38.2739	-108.8705	-1.2	2.7	0.2	3.3	near-well
4/6/15	8:34:50	38.2739	-108.8706	-1.2	2.7	-0.5	3.3	near-well
4/8/15	0:51:14	38.2705	-108.9332	-1.1	2.6	0.1	4.4	near-well
4/9/15	3:41:11	38.2772	-108.9260	-0.7	2.2	-0.4	3.5	near-well
4/16/15	5:35:46	38.2727	-108.8595	-2.1	3.6	-0.5	4.1	near-well
4/16/15	7:10:10	38.2702	-108.8655	-1.2	2.7	0.5	3.9	near-well
4/21/15	0:44:12	38.2625	-108.8687	1.4	0.1	0.4	4.4	near-well
4/22/15	2:07:16	38.2765	-108.9000	1.2	0.4	0.1	2.3	near-well
4/23/15	0:44:12	38.3325	-108.8615	-4.6	6.2	-0.3	5.0	central valley
4/26/15	6:20:31	38.2992	-108.8797	-4.5	6.0	-0.6	1.4	near-well
4/29/15	7:50:45	38.3089	-108.8910	-2.6	4.1	0.6	1.4	near-well
5/8/15	20:49:28	38.2693	-108.8690	-1.0	2.6	-0.8	3.8	near-well
5/11/15	4:53:11	38.2878	-108.8975	-2.4	3.9	-0.3	1.0	near-well
5/12/15	2:54:04	38.4051	-108.9300	-4.5	6.0	-0.2	12.4	N. valley
5/15/15	15:03:38	38.3089	-108.8912	-2.6	4.1	-0.5	1.4	near-well
5/18/15	4:28:20	38.2874	-108.8951	-2.2	3.7	0.3	1.0	near-well
5/20/15	11:12:42	38.2850	-108.9012	-1.6	3.1	-0.4	1.4	near-well
5/22/15	16:41:48	38.3238	-108.9704	-2.4	3.9	-0.3	7.3	NW cluster
5/23/15	3:37:27	38.2687	-108.8710	-0.2	1.7	0.0	3.7	near-well
5/24/15	13:25:42	38.2772	-108.8321	-2.2	3.8	0.7	5.9	SE cluster
5/25/15	4:05:45	38.2811	-108.8832	-3.3	4.8	0.2	2.0	near-well
5/25/15	12:06:17	38.3562	-108.8823	-5.4	6.9	0.2	6.7	central valley

Date	Time[1]	Latitude (deg.)	Longitude (deg.)	Elevation[2] (km)	Depth[3] (km)	M[4]	Distance from Injection Well (km)	Old Location Category[5]
6/3/15	9:39:25	38.3472	-108.8903	-4.2	5.7	0.8	5.6	central valley
6/11/15	0:02:35	38.2771	-108.8328	-2.2	3.7	-0.1	5.9	SE cluster
6/13/15	16:02:43	38.2838	-108.9050	-2.0	3.5	-0.8	1.7	near-well
6/14/15	5:40:43	38.2790	-108.8780	-5.3	6.8	-0.5	2.5	near-well
6/16/15	19:04:08	38.2815	-108.7988	-5.0	6.5	-0.2	8.6	other
6/18/15	7:41:28	38.2760	-108.8032	-2.7	4.2	0.2	8.4	other
6/21/15	9:16:51	38.2862	-108.8835	-2.0	3.5	0.1	1.5	near-well
6/21/15	11:19:28	38.2906	-108.9050	-2.0	3.5	-0.3	1.1	near-well
6/22/15	4:26:28	38.2808	-108.9390	-0.5	2.0	-0.1	4.2	near-well
6/24/15	9:58:33	38.2854	-108.9095	-1.7	3.3	-0.1	1.8	near-well
6/26/15	0:35:59	38.3060	-108.9043	-2.4	3.9	-0.3	1.3	near-well
6/27/15	5:12:04	38.3566	-108.8809	-5.4	6.9	-0.2	6.8	central valley
6/27/15	10:01:07	38.2902	-108.8829	-4.6	6.2	0.4	1.3	near-well
6/28/15	14:10:09	38.2840	-108.9057	-1.7	3.2	-0.1	1.7	near-well
6/28/15	14:15:37	38.2840	-108.9058	-1.7	3.2	0.9	1.7	near-well
6/28/15	15:00:03	38.2840	-108.9061	-1.7	3.2	-0.3	1.7	near-well
7/3/15	1:10:23	38.2758	-108.8998	0.6	0.9	0.2	2.3	near-well
7/3/15	3:55:49	38.2753	-108.9015	2.1	-0.6	-0.1	2.4	near-well
7/3/15	4:03:41	38.2778	-108.9020	1.9	-0.3	1.1	2.2	near-well
7/3/15	4:04:03	38.2745	-108.8997	2.3	-0.7	-0.6	2.5	near-well
7/8/15	17:08:45	38.2840	-108.9056	-1.7	3.2	-0.2	1.7	near-well
7/16/15	0:55:15	38.2323	-108.7772	-3.2	4.7	0.2	12.5	other
7/17/15	14:20:40	38.4072	-108.8677	-3.5	5.0	-0.4	12.5	N. valley
7/17/15	15:48:55	38.4057	-108.8700	-3.6	5.2	-0.9	12.3	N. valley
7/17/15	15:49:02	38.4075	-108.8682	-3.6	5.1	0.3	12.5	N. valley
7/17/15	15:50:22	38.4085	-108.8697	-3.4	4.9	-0.4	12.6	N. valley
7/17/15	23:56:11	38.4080	-108.8713	-3.6	5.1	-0.3	12.5	N. valley
7/18/15	10:12:30	38.3238	-108.9714	-2.1	3.7	0.3	7.3	NW cluster
7/21/15	11:02:51	38.4062	-108.8712	-3.4	5.0	0.2	12.3	N. valley
7/24/15	0:58:42	38.3563	-108.8819	-5.4	6.9	-0.4	6.7	central valley
7/26/15	18:11:31	38.2708	-108.8873	-1.8	3.3	-0.9	2.9	near-well
7/27/15	12:01:29	38.4078	-108.8647	-4.2	5.7	0.0	12.6	N. valley
7/28/15	1:32:08	38.2780	-108.8247	-2.5	4.0	-0.3	6.5	SE cluster
7/29/15	17:08:30	38.4087	-108.8647	-4.3	5.8	0.2	12.7	N. valley
8/2/15	8:50:09	38.3563	-108.8818	-5.4	6.9	0.9	6.7	central valley
8/4/15	23:46:26	38.4081	-108.8612	-3.7	5.2	0.4	12.7	N. valley
8/5/15	0:48:54	38.4085	-108.8613	-3.8	5.3	0.2	12.8	N. valley
8/10/15	7:26:34	38.3943	-108.9957	-5.0	6.5	0.3	14.0	N. valley
8/13/15	6:30:09	38.2747	-108.9250	0.1	1.4	-0.1	3.6	near-well
8/14/15	22:42:18	38.2865	-108.8844	-1.8	3.3	0.2	1.4	near-well
8/20/15	21:08:04	38.2002	-108.7248	-4.0	5.6	1.4	18.3	other
8/31/15	3:21:56	38.3332	-108.7620	-4.6	6.2	0.2	12.3	other

Date	Time[1]	Latitude (deg.)	Longitude (deg.)	Elevation[2] (km)	Depth[3] (km)	M[4]	Distance from Injection Well (km)	Old Location Category[5]
8/31/15	22:02:28	38.3318	-108.7665	-4.8	6.3	1.6	11.9	other
9/1/15	3:05:11	38.3014	-108.9307	-2.3	3.8	-0.1	3.2	near-well
9/4/15	4:39:12	38.2000	-108.7250	-4.0	5.6	1.0	18.3	other
9/9/15	1:50:22	38.2688	-108.9078	1.3	0.3	0.6	3.3	near-well
9/10/15	4:19:43	38.3068	-108.9147	-2.9	4.4	0.1	2.1	near-well
9/11/15	13:56:38	38.3068	-108.9148	-2.9	4.4	0.2	2.1	near-well
9/12/15	4:49:12	38.2856	-108.8937	-2.0	3.6	-0.1	1.2	near-well
9/14/15	15:28:07	38.2697	-108.8680	-0.9	2.4	-0.2	3.8	near-well
9/15/15	3:38:57	38.2707	-108.8659	-1.2	2.7	-0.1	3.8	near-well
9/17/15	22:32:18	38.2867	-108.9065	-3.6	5.1	-0.6	1.5	near-well
9/19/15	14:47:57	38.3239	-108.9710	-2.0	3.6	-0.5	7.3	NW cluster
9/27/15	10:10:13	38.2593	-108.8698	-1.3	2.8	0.1	4.7	near-well
9/30/15	20:25:08	38.2755	-108.8730	-2.1	3.6	-0.7	3.0	near-well
9/30/15	22:26:59	38.2750	-108.8745	-0.9	2.4	0.1	3.0	near-well
10/5/15	9:55:41	38.4088	-108.8615	-3.9	5.4	0.6	12.8	N. valley
10/5/15	11:47:53	38.4087	-108.8614	-3.8	5.4	0.3	12.8	N. valley
10/12/15	5:25:38	38.3167	-108.9734	-2.0	3.6	0.1	7.2	NW cluster
10/15/15	16:56:40	38.3317	-108.7643	-4.8	6.4	0.9	12.1	other
10/17/15	14:26:26	38.4385	-108.9550	-6.9	8.5	-0.3	16.6	N. valley
10/23/15	3:35:19	38.3089	-108.8911	-2.6	4.1	0.8	1.4	near-well
10/30/15	23:50:15	38.2868	-108.8833	-1.7	3.3	0.1	1.5	near-well
11/7/15	9:19:26	38.3015	-108.9304	-2.3	3.8	0.4	3.1	near-well
11/10/15	15:03:49	38.4388	-108.9557	-7.2	8.7	0.0	16.7	N. valley
11/14/15	2:36:03	38.2839	-108.9086	-1.7	3.2	1.0	1.8	near-well
11/14/15	19:52:34	38.4688	-109.0505	-2.0	3.5	0.2	23.5	N. valley
11/14/15	21:20:09	38.4377	-108.9538	-6.9	8.4	-0.2	16.5	N. valley
11/15/15	9:03:31	38.2840	-108.9083	-1.6	3.2	-0.2	1.8	near-well
11/19/15	7:37:15	38.3342	-108.7677	-4.8	6.3	1.3	11.9	other
11/21/15	5:39:10	38.4028	-108.8656	-3.5	5.0	0.5	12.1	N. valley
11/22/15	6:38:34	38.2846	-108.9032	-1.7	3.2	0.7	1.5	near-well
11/22/15	6:58:34	38.2846	-108.9033	-1.7	3.2	-0.5	1.5	near-well
11/27/15	3:49:37	38.2668	-108.8793	-0.8	2.3	-0.3	3.6	near-well
11/27/15	5:54:52	38.3188	-108.8167	-4.0	5.5	-0.5	7.3	other
12/3/15	11:00:32	38.2887	-108.9002	-2.5	4.0	-0.9	1.0	near-well
12/9/15	5:03:24	38.4053	-108.9319	-4.5	6.0	-0.3	12.5	N. valley
12/12/15	22:47:03	38.3277	-108.7447	-3.7	5.3	0.3	13.6	other
12/13/15	23:40:13	38.3276	-108.7446	-3.7	5.3	0.3	13.6	other
12/15/15	2:37:54	38.2667	-108.9447	-0.8	2.3	-0.3	5.5	near-well
12/17/15	5:27:22	38.2770	-108.8770	-1.0	2.5	-0.1	2.7	near-well
12/17/15	11:06:16	38.3060	-108.9156	-3.0	4.5	-0.1	2.1	near-well
12/17/15	11:06:53	38.3170	-108.9130	-4.1	5.6	-1.1	2.8	near-well
12/18/15	0:41:33	38.2852	-108.9004	-1.7	3.2	-0.2	1.3	near-well
12/21/15	10:39:40	38.3277	-108.7445	-3.7	5.3	0.8	13.6	other
12/28/15	9:46:04	38.2705	-108.8783	-0.7	2.2	0.0	3.2	near-well
12/28/15	18:43:59	38.2851	-108.9000	-2.1	3.6	0.1	1.3	near-well
12/29/15	1:57:43	38.3305	-108.7577	-3.8	5.4	0.1	12.6	other
12/29/15	2:38:45	38.3367	-108.7658	-3.7	5.2	0.0	12.1	other

Date	Time[1]	Latitude (deg.)	Longitude (deg.)	Elevation[2] (km)	Depth[3] (km)	M[4]	Distance from Injection Well (km)	Old Location Category[5]
12/29/15	21:58:12	38.2990	-108.9005	-2.5	4.1	-0.2	0.6	near-well
12/29/15	21:58:42	38.2986	-108.9002	-2.5	4.1	-0.6	0.5	near-well

[1] Time listed is Coordinated Universal Time, UTC (Mountain Standard Time = UTC – 7 hours; Mountain Daylight Savings Time = UTC – 6 hours)
[2] Elevation is given with respect to mean sea level.
[3] Depth is referenced to the surveyed ground surface elevation at the injection wellhead, 1.524 km.
[4] Magnitudes listed are duration magnitudes, unless specified otherwise
[5] Earthquake location categories:

- near-well: located within approximately 5 km of the injection well
- northwest cluster (abbrev. “NW cluster”): located within the zone of induced seismicity that is centered approximately 7.5 km northwest of the injection well
- southeast cluster (abbrev. “SE cluster”): located approximately 6 km southeast of the injection well
- central valley: located within north-central Paradox Valley
- northern valley (abbrev. “N. valley”): located in or very near areas of recurring seismicity along the northern edges of Paradox Valley
- other: local earthquake not associated with any other location category, or locating deeper than 8 km